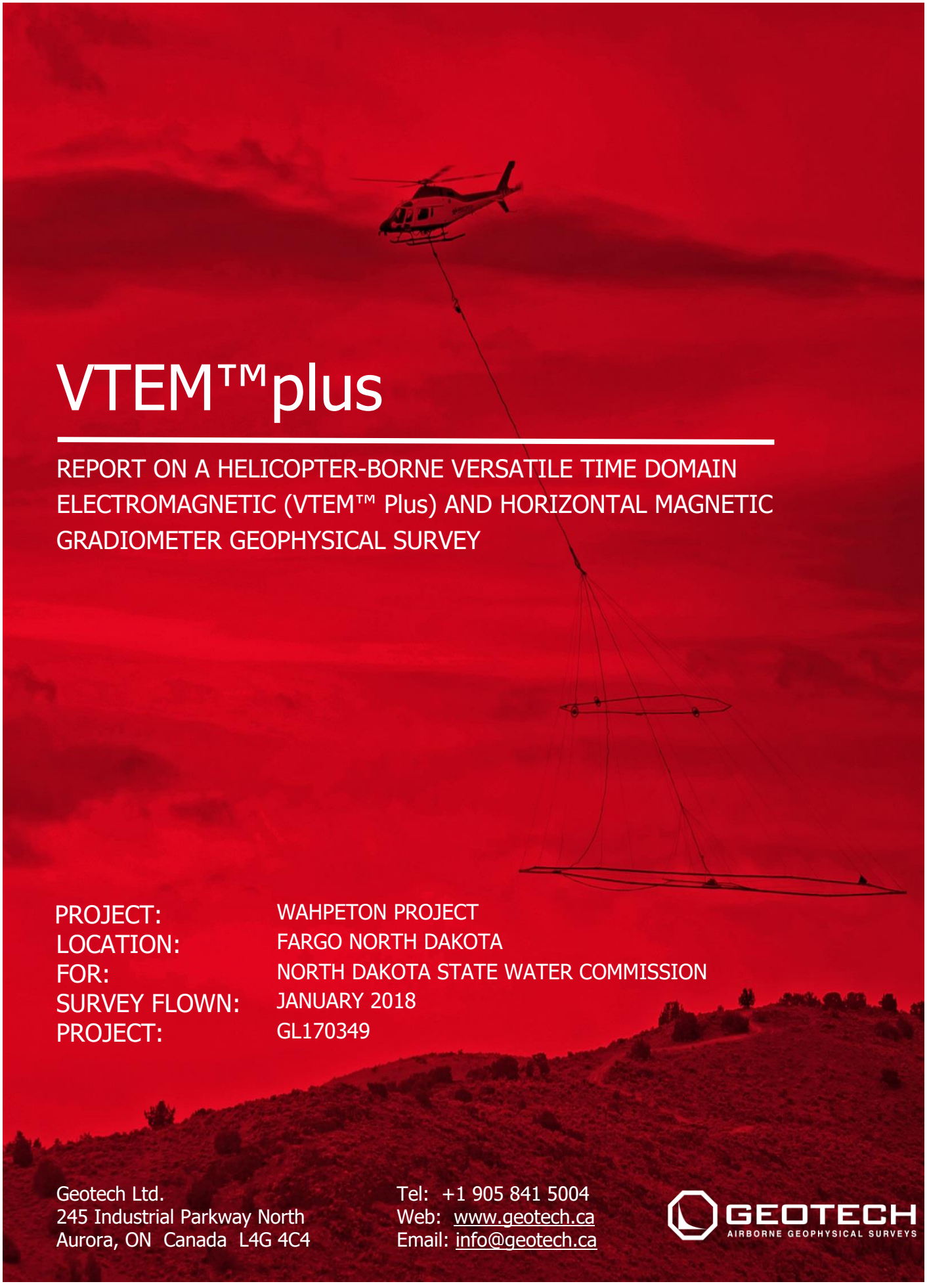

VTEM™plus

REPORT ON A HELICOPTER-BORNE VERSATILE TIME DOMAIN ELECTROMAGNETIC (VTEM™ Plus) AND HORIZONTAL MAGNETIC GRADIOMETER GEOPHYSICAL SURVEY

PROJECT:	WAHPETON PROJECT
LOCATION:	FARGO NORTH DAKOTA
FOR:	NORTH DAKOTA STATE WATER COMMISSION
SURVEY FLOWN:	JANUARY 2018
PROJECT:	GL170349

Geotech Ltd.
245 Industrial Parkway North
Aurora, ON Canada L4G 4C4

Tel: +1 905 841 5004
Web: www.geotech.ca
Email: info@geotech.ca

GEOTECH
AIRBORNE GEOPHYSICAL SURVEYS

TABLE OF CONTENTS

LIST OF FIGURES

LIST OF TABLES

APPENDICES

EXECUTIVE SUMMARY

WAHPETON PROJECT
FARGO, NORTH DAKOTA

During November 6th to 19th, 2017 Geotech Ltd. carried out a helicopter-borne geophysical survey over the Wahpeton Project situated near Fargo, North Dakota.

Principal geophysical sensors included a versatile time domain electromagnetic (VTEM™plus) system and a horizontal magnetic gradiometer with two caesium sensors. Ancillary equipment included two GPS navigation systems, a radar altimeter, and a gyroscopic inclinometer. A total of 2000 line-kilometres of geophysical data were acquired during the survey.

In-field data quality assurance and preliminary processing were carried out on a daily basis during the acquisition phase. Preliminary and final data processing, including generation of final digital data and map products were undertaken from the office of Geotech Ltd. in Aurora, Ontario.

The processed survey results are presented as the following maps:

- Electromagnetic stacked profiles of the B-field Z Component,
- Electromagnetic stacked profiles of dB/dt Z Components,
- B-Field Z Component Channel grid,
- Total Magnetic Intensity (TMI),
- Magnetic Total Horizontal Gradient,

The final processed data was inverted to create 1D resistivity models over the entire survey block. The inversions were performed by Geotech and by Aqua Geo Frameworks. The inversion results were effective at mapping aquifer material in the Fargo-Wahpeton project area. These results are presented as:

- Planar resistivity depth slices
- Cross-sectional resistivity models for each flight and tie line
- 3D gridded voxel composed from each 1D inversion model

Digital data includes all electromagnetic and magnetic products, plus ancillary data including the waveform and all inversion modeling products.

The survey report describes the procedures for data acquisition, processing, final image presentation, inversion modeling, and the specifications for the digital data set.

Aqua Geo Frameworks produced a separate report describing their data processing workflow and 1D inversions results. The Aqua Geo Frameworks report and technical products are part of the project deliverables.

1. INTRODUCTION

1.1 GENERAL CONSIDERATIONS

Geotech Ltd. performed a helicopter-borne geophysical survey over the Wahpeton Project situated near Fargo, North Dakota (Figure 1 & Figure 2).

Jon Patch represented North Dakota State Water Commission during the data acquisition, data processing, and data modeling phases of this project

The geophysical surveys consisted of helicopter borne EM using the versatile time-domain electromagnetic (VTEM) plus system with Full-Waveform processing. Measurements consisted of Vertical (Z), In-line Horizontal (X), and Cross-line Horizontal (Y) components of the EM fields using induction coils and the aeromagnetic total field using two caesium magnetometers. A total of 2000 line-km of geophysical data were acquired during the survey.

The crew was based out of Fargo (Figure 2) in North Dakota for the acquisition phase of the survey. Survey flying started on November 6th and was completed on November 19th, 2017.

Figure 1: Survey location

Data quality control and quality assurance, and preliminary data processing were carried out on a daily basis during the acquisition phase of the project. Aqua Geo Frameworks performed additional quality control and preliminary 1D inversion on the acquired EM data.

Final data processing followed immediately after the end of the survey. Final reporting, data presentation, data modeling and archiving were completed from the Aurora office of Geotech Ltd. in January, 2017. A set of unconstrained 1D layered earth inversions (LEI) were produced by Geotech while Aqua Geo Frameworks performed laterally constrained inversions (LCI) and spatially constrained inversions (SCI) on the final processed dataset.

1.2 SURVEY AND SYSTEM SPECIFICATIONS

The survey area is located west of Fargo, North Dakota (Figure 2).

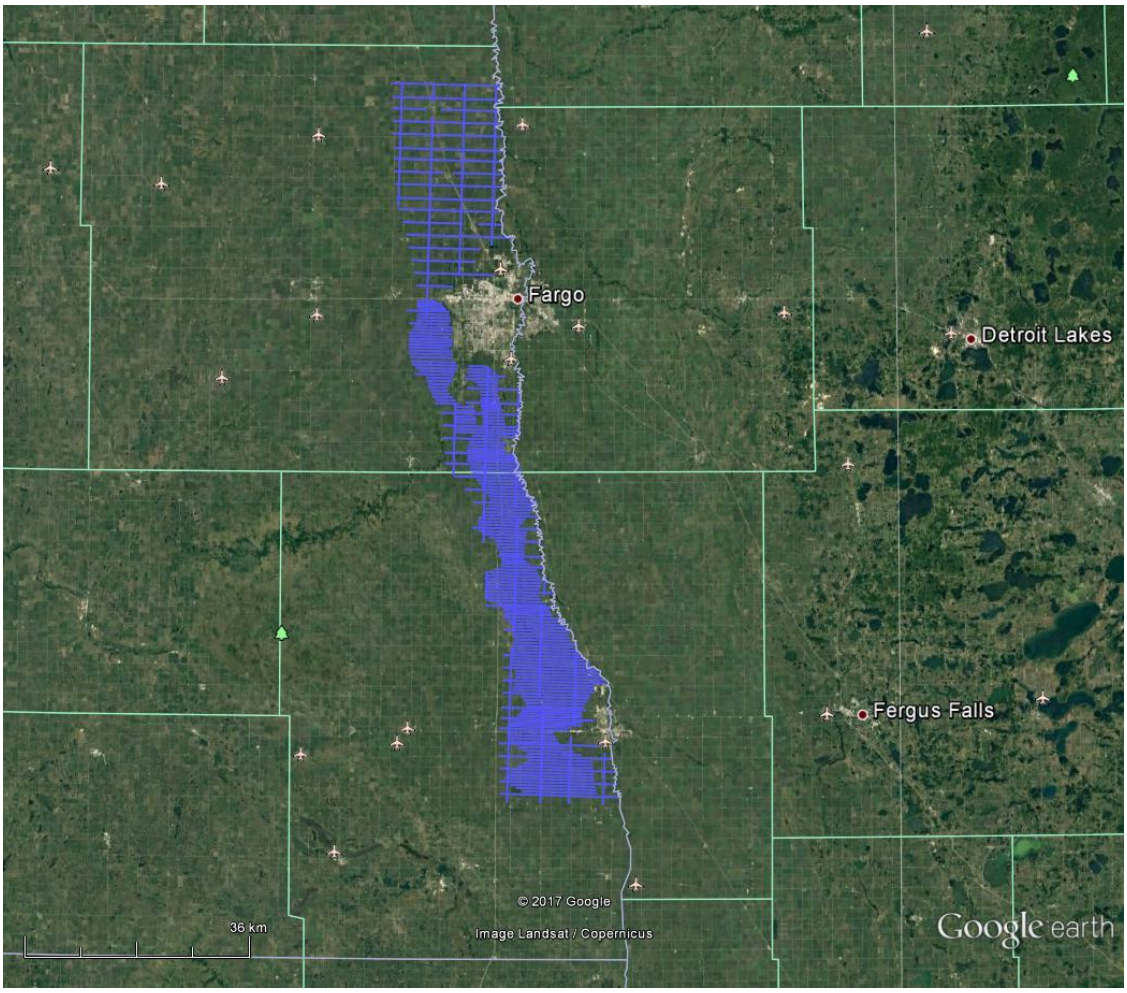

Figure 2: Survey area location on Google Earth.

The survey area was flown in an east to west (N 90° E azimuth) direction with traverse line spacings of 500 and 2000 metres as depicted in Figure 3. Tie lines were flown perpendicular to the traverse lines

For more detailed information on the flight spacing and direction see Table 1.

1.3 TOPOGRAPHIC RELIEF AND CULTURAL FEATURES

Topographically, the survey area exhibits a shallow relief with an elevation ranging from 256 - 302 metres above mean sea level over an area of 1370 square kilometres (Figure 3).

There are various rivers and streams running through the survey area which connect various lakes. There are visible signs of culture such as roads, railways and settlements located in and around the survey area.

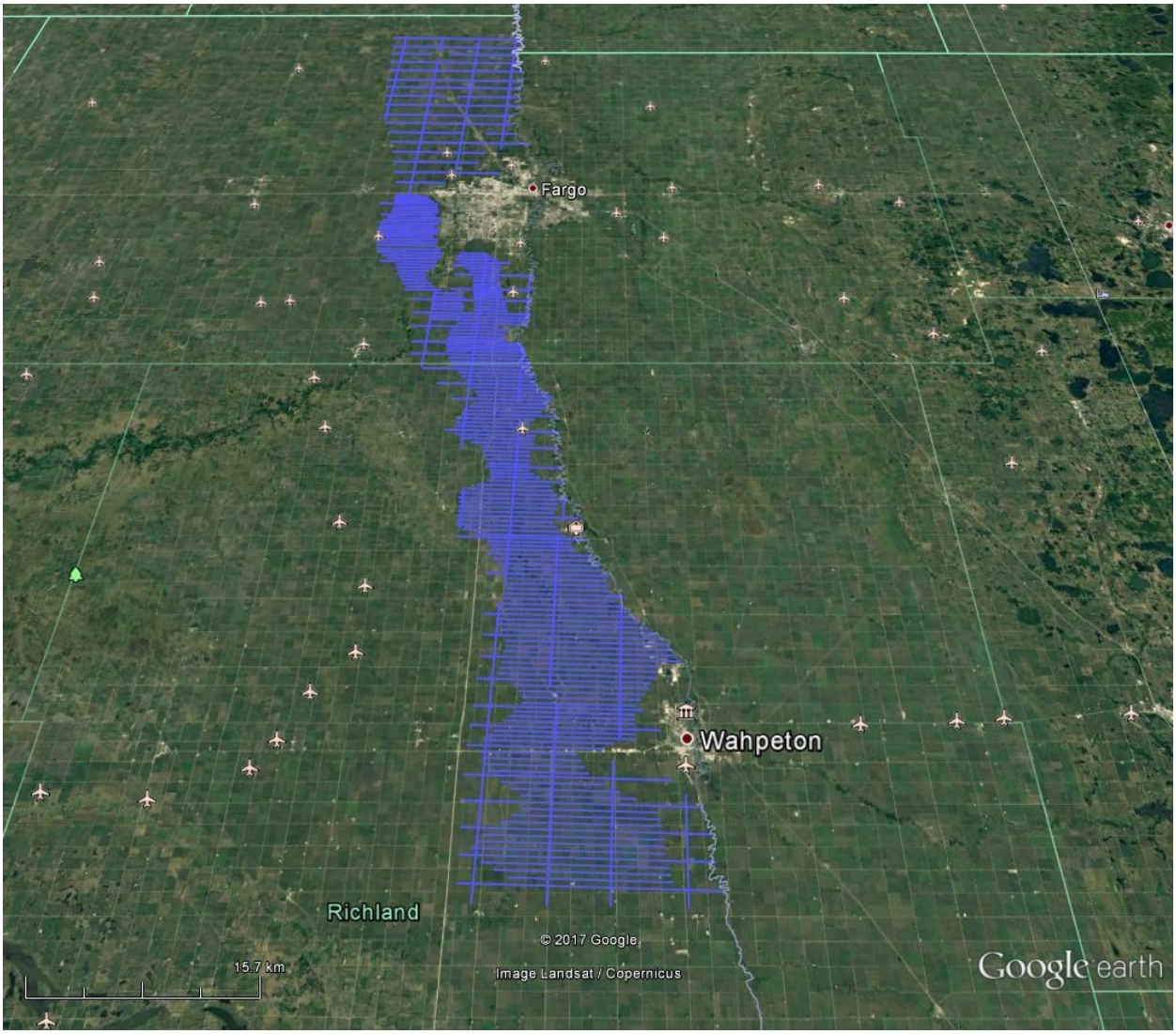

Figure 3: Flight path over a Google Earth Image.

2. DATA ACQUISITION

2.1 SURVEY AREA

The survey area (see Figure 3 and Appendix A) and general flight specifications are as follows:

Table 1: Survey Specifications

Survey block	Line spacing (m)	Area (Km^2)	Planned[1] Line-km	Actual Line-km	Flight direction	Line numbers
Wahpeton	Traverse: 500 & 2000	1370	2000	2073	N 90° E / N 270° E	L1000 – L1560
	Tie: 5000				N 0° E / N 180° E	L3000 – L3070

Additional data was provided to the NDSWC as the lead-in (~100m) and lead-out (~100m) for each planned survey line. For this reason the delivered data contains more data than planned.

Survey area boundaries co-ordinates are provided in Appendix B.

2.2 SURVEY OPERATIONS

Survey operations were based out of Fargo, North Dakota from November 6th to 19th, 2017. The following table shows the timing of the flying.

Table 2: Survey schedule

Date	Flight #	Flown km	Block	Crew location	Comments
6-Nov-2017				Fargo, North Dakota	Meeting with FAA in the morning, maintenance checks on Heli. Attempted test flight but found issue with system, troubleshoot and repair system. Another test flight attempted in the afternoon but aborted due to weather.
7-Nov-2017	1	20		Fargo, North Dakota	Completed system testing, test flight included 1 line, 20km flown. System is ready for production.
8-Nov-2017	2, 3, 4	304		Fargo, North Dakota	307km flown
9-Nov-2017	5, 6, 7	275		Fargo, North Dakota	275km flown
10-Nov-2017				Fargo, North Dakota	No production due to weather, high winds throughout the day.
11-Nov-2017	8, 9	162		Fargo, North Dakota	162km flown
12-Nov-2017	10, 11, 12	331		Fargo, North Dakota	Low ceiling in the morning, 331km flown
13-Nov-2017	13, 14	269		Fargo, North Dakota	269km flown
14-Nov-2017				Fargo, North Dakota	No production due to weather, fog.
15-Nov-2017				Fargo, North Dakota	No production due to weather, low ceiling and strong winds.
16-Nov-2017				Fargo, North Dakota	No production due to weather, low ceiling and strong winds.

[1] Note: Actual Line kilometres represent the total line kilometres in the final database. These line-km normally exceed the Planned Line-km, as indicated in the survey NAV files.

Date	Flight #	Flown km	Block	Crew location	Comments
17-Nov-2017	15, 16, 17	355		Fargo, North Dakota	355km flown.
18-Nov-2017	18, 19, 20	284		Fargo, North Dakota	283km flown, flight path complete
19-Nov-2017				Fargo, North Dakota	Commence Demobilization

2.3 PROCEDURES

The on board operator was responsible for monitoring the system integrity. He also maintained a detailed flight log during the survey, tracking the times of the flight as well as any unusual geophysical or topographic features.

On return of the aircrew to the base camp the survey data was transferred from a compact flash card (PCMCIA) to the data processing computer. The data were then uploaded via ftp to the Geotech office in Aurora for daily quality assurance and quality control by qualified personnel.

2.4 AIRCRAFT AND EQUIPMENT

2.4.1 SURVEY AIRCRAFT

The survey was flown using a Eurocopter Aerospatiale (Astar) 350 B3 helicopter, registration C-GEOC. The helicopter is owned and operated by Geotech Aviation. Installation of the geophysical and ancillary equipment was carried out by a Geotech Ltd crew.

2.4.2 ELECTROMAGNETIC SYSTEM

The electromagnetic system was a Geotech Time Domain EM (VTEM™plus) full receiver-waveform streamed data recorded system. The "full waveform VTEM system" uses the streamed half-cycle recording of transmitter and receiver waveforms to obtain a complete system response calibration throughout the entire survey flight. VTEM with the Serial number 31 was used for the survey. The VTEM™ transmitter current waveform is shown diagrammatically in Figure 4.

The VTEM™ Receiver and transmitter coils were in concentric-coplanar and Z-direction oriented configuration. The receiver system for the project also included coincident-coaxial X-direction and Y-direction coils to measure the in-line and cross-line dB/dt and calculate B-Field responses, respectively. The transmitter-receiver loop was towed at a mean distance of 35 metres below the aircraft as shown in Figure 5.

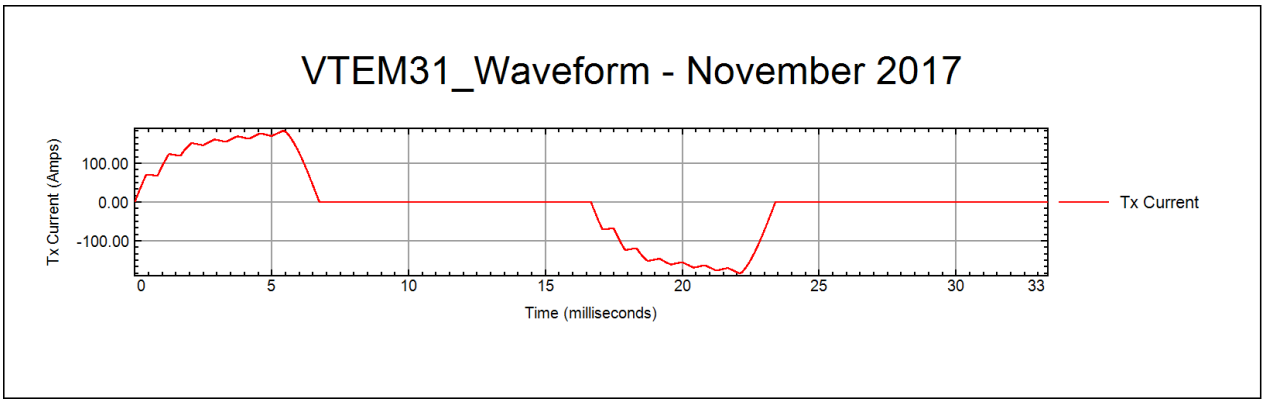

Figure 4: VTEM™ Transmitter Current Waveform

The VTEM™ decay sampling scheme is shown in Table 3 below. Forty-three time measurement gates were used for the final data processing in the range from 0.021 to 8.083 msec. Zero time for the off-time sampling scheme is equal to the current pulse width and is defined as the time near the end of the turn-off ramp where the dI/dt waveform falls to 1/2 of its peak value.

Table 3: Off-Time Decay Sampling Scheme

VTEM™ Decay Sampling Scheme				
Index	Start	End	Middle	Width
Milliseconds				
4	0.018	0.023	0.021	0.005
5	0.023	0.029	0.026	0.005
6	0.029	0.034	0.031	0.005
7	0.034	0.039	0.036	0.005
8	0.039	0.045	0.042	0.006
9	0.045	0.051	0.048	0.007
10	0.051	0.059	0.055	0.008
11	0.059	0.068	0.063	0.009
12	0.068	0.078	0.073	0.010
13	0.078	0.090	0.083	0.012
14	0.090	0.103	0.096	0.013
15	0.103	0.118	0.110	0.015
16	0.118	0.136	0.126	0.018
17	0.136	0.156	0.145	0.020
18	0.156	0.179	0.167	0.023
19	0.179	0.206	0.192	0.027
20	0.206	0.236	0.220	0.030
21	0.236	0.271	0.253	0.035
22	0.271	0.312	0.290	0.040
23	0.312	0.358	0.333	0.046
24	0.358	0.411	0.383	0.053
25	0.411	0.472	0.440	0.061

VTEM™ Decay Sampling Scheme				
Index	Start	End	Middle	Width
Milliseconds				
26	0.472	0.543	0.505	0.070
27	0.543	0.623	0.580	0.081
28	0.623	0.716	0.667	0.093
29	0.716	0.823	0.766	0.107
30	0.823	0.945	0.880	0.122
31	0.945	1.086	1.010	0.141
32	1.086	1.247	1.161	0.161
33	1.247	1.432	1.333	0.185
34	1.432	1.646	1.531	0.214
35	1.646	1.891	1.760	0.245
36	1.891	2.172	2.021	0.281
37	2.172	2.495	2.323	0.323
38	2.495	2.865	2.667	0.370
39	2.865	3.292	3.063	0.427
40	3.292	3.781	3.521	0.490
41	3.781	4.341	4.042	0.560
42	4.341	4.987	4.641	0.646
43	4.987	5.729	5.333	0.742
44	5.729	6.581	6.125	0.852
45	6.581	7.560	7.036	0.979
46	7.560	8.685	8.083	1.125

Z Component: 4 - 46 time gates
X Component: 20 - 46 time gates
Y Component: 20 - 46 time gates

VTEM™ system specifications:

Transmitter	Receiver
• Transmitter loop diameter: 26 m • Number of turns: 4 • Effective Transmitter loop area: 2123.7 m^2 • Transmitter base frequency: 30 Hz • Peak current: 183.2 A • Pulse width: 6.73 ms • Waveform shape: Bi-polar trapezoid • Peak dipole moment: 389,062 nIA • Average transmitter-receiver loop terrain clearance: 36 metres above the ground	• X Coil diameter: 0.32 m • Number of turns: 245 • Effective coil area: 19.69 m^2 • Y Coil diameter: 0.32 m • Number of turns: 245 • Effective coil area: 19.69 m^2 • Z-Coil diameter: 1.2 m • Number of turns: 100 • Effective coil area: 113.04 m^2

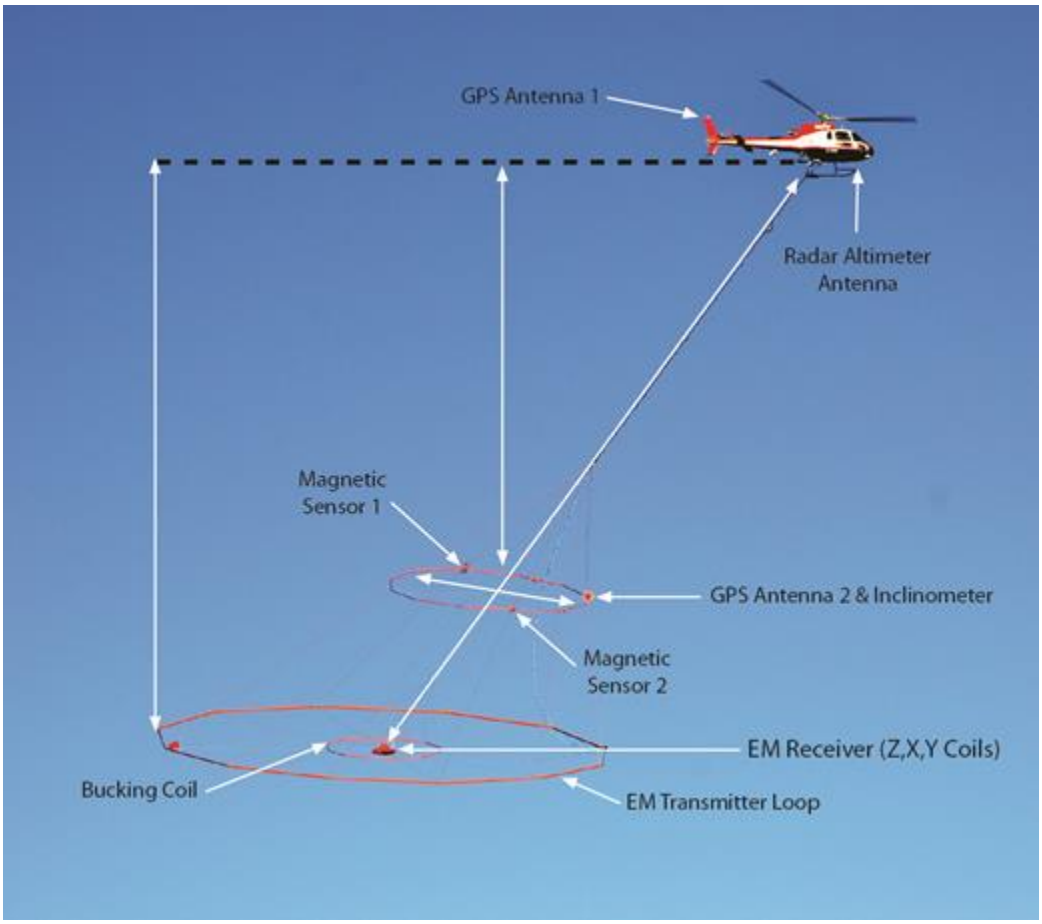

Figure 5: VTEM™Plus System Configuration.

2.4.3 FULL WAVEFORM VTEM™ SENSOR CALIBRATION

The calibration is performed with the completely assembled VTEM system connected to the helicopter at the survey site on the ground. Measurements of the half-cycles are collected and used to calculate a sensor calibration consisting of a single stacked half-cycle waveform. The purpose of the stacking is to attenuate natural and man-made magnetic signals, leaving only the response to the calibration signal. The stacked half-cycle allows the transfer functions between the receiver and data acquisition system, $H_D(\omega)$, and current sensor and data acquisition system, $H_R(\omega)$, to be determined. These transfer functions are used as a part of the system response correction during processing to correct the half-cycle waveforms and data acquired on a survey flight to a common transfer function:

$$D(\omega) = [H_C(\omega)/H_D(\omega)]\, D_R(\omega)$$
$$A(\omega) = [H_C(\omega)/H_R(\omega)]\, A_R(\omega)$$

where $H_C(\omega)$ is the common transfer function, and $D_R(\omega)$ and $A_R(\omega)$ are the FFT's of the raw receiver and current sensor responses recorded by the data acquisition system.

This process allows for the receiver response, R(ω), to become independent of the sensor characteristics determined by the transfer functions $H_D(\omega)$ and $H_R(\omega)$ and acts similar to a deconvolution of the data.

$$R(\omega) = \frac{D(\omega)I(\omega)}{A(\omega)}$$

where, D(ω) is the FFT of the actual receiver data sample D(t), I(ω) is the FFT of a reference or "Ideal waveform" and A(ω) is the FFT of the actual waveform.

2.4.4 Horizontal Magnetic Gradiometer

The horizontal magnetic gradiometer consists of two Geometrics split-beam field magnetic sensors with a sampling interval of 0.1 seconds. These sensors are mounted 12.5 metres apart on a separate loop, 9 metres above the Transmitter-receiver loop. A GPS antenna and Gyro Inclinometer is installed on the separate loop to accurately record the tilt and position of the magnetic gradiomag bird.

2.4.5 GPS Navigation System

The navigation system used was a Geotech PC104 based navigation system utilizing a NovAtel's WAAS (Wide Area Augmentation System) enabled GPS receiver, Geotech navigate software, a full screen display with controls in front of the pilot to direct the flight and a NovAtel GPS antenna mounted on the helicopter tail (Figure 5). As many as 11 GPS and two WAAS satellites may be monitored at any one time. The positional accuracy or circular error probability (CEP) is 1.8 m, with WAAS active, it is 1.0 m. The co-ordinates of the survey area were set-up prior to the survey and the information was fed into the airborne navigation system. The second GPS antenna is installed on the additional magnetic loop together with Gyro Inclinometer.

2.4.6 GPS - Magnetic-Gradiometer Loop

A NovAtel GPS antenna was installed on the front centre of the magnetic gradiometer loop to accurately record the position of the loop (Figure 5). GPS data were sampled every 0.1 seconds. The final GPS coordinates were differentially corrected by post-processing the gradiometer loop data along with GPS data obtained simultaneously from a base station setup nearby the survey area. Final horizontal coordinates are referenced to WGS84 UTM zone 14N and the height is referenced to the geoid. The positional accuracy or circular error probability (CEP) is 1.0 m.

2.4.7 Inclinometer – Magnetic Gradiometer Loop

An Anlalog Devices ADIS16405 gyroscopic inclinometer was installed on the magnetic gradiometer loop (Figure 5) to accurately record the orientation of the loop with a sampling interval of 0.1 seconds.

2.4.8 Radar Altimeter

A Terra TRA 3000/TRI 40 radar altimeter was used to record terrain clearance. The antenna was mounted beneath the bubble of the helicopter cockpit (Figure 5).

2.4.9 VIDEO CAMERA

A Garmin VIRB®X camera was used which captures high-definition, wide-angle footage at 1080p30, 12 megapixel photos at 10 frames per second.

2.4.10 DIGITAL ACQUISITION SYSTEM

A Geotech data acquisition system recorded the digital survey data on an internal compact flash card. Data is displayed on an LCD screen as traces to allow the operator to monitor the integrity of the system. The data type and sampling interval as provided in Table 4.

Table 4: Acquisition Sampling Rates

Data Type	Sampling
TDEM	0.1 sec
Magnetometer	0.1 sec
GPS Position	0.1 sec
Radar Altimeter	0.2 sec
Inclinometer	0.2 sec

2.5 BASE STATION

A combined magnetometer/GPS base station was utilized on this project. A Geometrics Caesium vapour magnetometer was used as a magnetic sensor with a sensitivity of 0.001 nT. The base station was recording the magnetic field together with the GPS time at 1 Hz on a base station computer.

The base station magnetometer sensor was installed at the Fargo Airport (46°56.9116' N, 98°48.9109' W); away from electric transmission lines and moving ferrous objects such as motor vehicles. The base station data were backed-up to the data processing computer at the end of each survey day.

3. PERSONNEL

The following Geotech Ltd. personnel were involved in the project.

FIELD:

Project Manager:	Shauna-Lee Hewitt (Office)
Data QC:	Dmitriy Danchenko (Office)
Crew chief:	Paul Taylor
Operator:	Scott Taylor

The survey pilot and the mechanical engineer were employed directly by the helicopter operator – Geotech Aviation.

Pilot:	Paul Winiecki
Mechanical Engineer:	n/a

OFFICE:

Preliminary Data Processing:	Dmitriy Danchenko
Final Data Processing:	Keeme Mokubung
Final Data QA/QC:	Zihao Han & Geoffrey Plastow
Final Data Modeling:	Nasreddine Bournas
Reporting/Mapping:	Kyle Orlowski

Processing and Interpretation phases were carried out under the supervision of Alexander Prikhodko, P.Geo, PhD, and Director of Geophysics. The customer relations were looked after by Jean Legault.

4. DATA PROCESSING AND PRESENTATION

Data compilation and processing were carried out by the application of Geosoft OASIS Montaj and programs proprietary to Geotech Ltd.

4.1 FLIGHT PATH

The flight path, recorded by the acquisition program as WGS 84 latitude/longitude, was converted into the WGS84 Datum, UTM Zone 14 North coordinate system in Oasis Montaj.

Both sets of GPS coordinate, from helicopter GPS and magnetic gradiometer GPS, were sampled every 0.1 seconds. A GPS base station, located at the locations listed in Section 2.5 was used in the Differential GPS (DGPS) post-processing of both sets of GPS coordinates. The confidence level of the post-processed DGPS coordinates is excellent for both the helicopter and gradiometer loop GPS based off mean HDOP of 0.91 and 0.92 and PDOP of 1.66 and 1.62, respectively.

The final set of coordinates were then calculated for the position halfway between the two magnetometers that are located on the left and right hand sides of the magnetic gradiometer loop. This position represents the centre of the magnetic gradiomter loop and is the point where the tow cable intersects the plane of the magnetic gradiometer loop. This was achieved by projecting backwards along the flight line by 6.25 m, the radius of the gradiometer loop, from the gradiometer loop GPS antenna position. The EM and magnetic data have been parallax corrected to this set of coordinates and to which all EM and magnetic data and interpretations should be referred.

4.2 CALCULATION OF EM TRANSMITTER RECEIVER LOOP HEIGHT

The EM transmitter-receiver loop height above ground was calculated using the differentially corrected gradiometer loop GPS and derived DEM data. The derived DEM was calculated using the helicopter GPS elevation and radar altimeter measurements, factoring in the vertical separation between the two sensors on the helicopter. This calculated DEM was then corrected to the National Elevation Dataset (NED) over the survey block by removing any linear trends between the two DEM values. The correction of the measured DEM to NED removes first-order errors that could have resulted from the radar altimeter measurement or variations in the quality of the GPS elevation measurements. The EM transmitter-receiver loop height above ground was calculated from the difference between this corrected DEM and the centre of the gradiometer loop elevation accounting for the vertical separation between the gradiometer and EM transmitter-receiver loop using a constant value of 9 metres.

4.3 ELECTROMAGNETIC DATA

As the data are acquired by the data acquisition system on the helicopter, it goes through a digital filter to reject major sferic events and is stacked to further reduce system noise. Afterward, the streamed data is processed by applying a system response correction, B-field integration, time window binning, compensation, filtering, and leveling. Three stages of processing of the EM data have been delivered. They are denoted in the final point-located EM dataset (Table 5) as;

1. Raw (Raw),
2. Filtered (Filt)
3. Final (F).

The digital filtering process is a three stage filter used to reject major sferic events and reduce system noise. Local sferic activity can produce sharp, large amplitude events that cannot be removed by conventional filtering procedures. Smoothing or stacking will reduce their amplitude but leave a broader residual response that can be confused with geological phenomena. To avoid this possibility, a computer algorithm searches out and rejects the major sferic events. The data was then stacked using 15 half cycles, 0.3 seconds, to create a stacked half-cycle waveform at 0.1 second intervals. The stacking coefficients are tapered with a shape that approximates a Gaussian function.

During post-flight processing, the streamed data have a sensor response correction applied which corrects the receiver channels and current monitor to a common impulse response based on the Full Waveform calibration (see Section 2.4.3). The B-field data are calculated by integrating the dB/dt cycles from the 192 kHz streamed data. Then, the streamed data are converted into a set of time window channels (see Table 3) to reduce noise levels further. The output of this stage is the data denoted as “Raw” in Table 5.

The data have noise levels reduced further by the use of an EM compensation procedure which removes characteristic noise from each fiducial determined by the difference between the transmitter and bucking loop fields at the receiver during the flight. This is achieved by a statistical correlation between each time window channel and primary field measurement taken during the on-time. Next, filtering of the electromagnetic data was performed in two steps. The first is a 5 fiducial wide non-linear filter to eliminate any large spikes remaining in the dataset. The second filter is a low pass symmetric linear digital filter that has zero-phase shift which prevents any lag or peak displacement from occurring, and it suppresses only variations with a wavelength less than about 1.5 second or around 40 metres. The data channels which have been processed to this point are denoted by “Filtered” in Table 5.

A “zero level” estimate was subtracted from the data at each fiducial to remove the remaining system response from the data. The “zero level” correction applied was calculated by linear interpolation of the high altitude backgrounds recorded two or more times during each survey flight. Afterwards, a parallax correction was applied to the EM data to account for the distance by which the EM transmitter-receiver loop lags behind the centre of the magnetic gradiometer loop. In this parallax correction the EM data are shuffled toward lower fiducial numbers by the nearest integer number of fiducials that it would take to travel the average horizontal distance which separates the centres of the magnetic gradiometer and EM loops based on the average helicopter speed for each line. This produces the EM data denoted as “Final” in Table 5.

VTEM™ has three receiver coil orientations. Z-axis coil is oriented parallel to the transmitter coil axis and both are horizontal to the ground. The X-axis coil is oriented parallel to the ground and along the line-of-flight. The Y-axis coil is oriented parallel to the ground and perpendicular to the line-of-flight. This combined three coil configuration provides information on the position, depth, dip and thickness of a conductor. Generalized modeling results of VTEM data, are shown in Appendix D.

In general X-component data produce cross-over type anomalies: from "+ to – "in flight direction of flight for "thin" sub vertical targets and from "- to +" in direction of flight for "thick" targets. Z component data produce double peak type anomalies for "thin" sub vertical targets and single peak for "thick" targets.

4.4 HORIZONTAL MAGNETIC GRADIOMETER DATA

The horizontal gradients data from the VTEM™Plus are measured by two magnetometers 12.5 m apart on an independent bird mounted 10m above the VTEM™ loop. A GPS and a Gyro Inclinometer help to determine the positions and orientations of the magnetometers. The data from the two magnetometers are corrected for position and orientation variations, as well as for the diurnal variations using the base station data.

The position of the centre of the horizontal magnetic gradiometer bird is calculated form the GPS utilizing in-house processing tool in Geosoft. Following that total magnetic intensity is calculated at the center of the bird by calculating the mean values from both sensors. In addition to the total intensity advanced processing is done to calculate the in-line and cross-line (or lateral) horizontal gradient which enhance the understanding of magnetic targets. The in-line (longitudinal) horizontal gradient is calculated from the difference of two consecutive total magnetic field readings divided by the distance along the flight line direction, while the cross-line (lateral) horizontal magnetic gradient is calculated from the difference in the magnetic readings from both magnetic sensors divided by their horizontal separation.

Two advanced magnetic derivative products, the total horizontal derivative (THDR), and tilt angle derivative and are also created. The total horizontal derivative or gradient is defined as:

THDR = sqrt(Hx*Hx+Hy*Hy), where Hx and Hy are cross-line and in-line horizontal gradients.

The tilt angle derivative (TDR) is defined as:

TDR = arctan(Vz/THDR), where THDR is the total horizontal derivative, and Vz is the vertical derivative.

Measured cross-line gradients can help to enhance cross-line linear features during gridding.

5. 1D INVERSION MODELS

The final processed data was used as the input modeling over the entire block. The algorithm used for the inversion modeling was GALEISBSTDEM[2] which is a one dimensional (1D) layered earth deterministic algorithm designed to invert airborne time-domain electromagnetic data. Since the algorithm is 1D, it assumes that the Earth is horizontally stratified and laterally-uniform layer conductivities and thicknesses. For VTEM, the 1D assumption works well in a stratified geology due to the limited lateral sensitivity of the system's measurement outside of its footprint[3]. Each of these 1D inversion models can be "stitched" together to form visualizations of the layer conductivities along the flight line in 2D and for the entire block in 3D.

The GALEISBSTDEM algorithm has two modeling options: a multi-layer smooth model which solves for the layer's conductivity while the thicknesses remain fixed, or a few-layer blocky model which solves for both the layer's conductivity and thickness. Since the inversion problem for AEM is under-determined, the solution is non-unique and regularization is needed to constrain the model results. The multi-layer smooth model constrains the inversion by fitting only smoothly varying conductivity models with respect to depth which acts as a way to regularize the results. The main constraint for a few-layer blocky model is the number of initial layers in the reference model since this option attempts to resolve a model that reflects the conductivity and thickness of each geological layer. The multi-layer smooth model option works best when there is little prior information about the expected model results due to the smooth nature of the regularization. However, this option is not able to accurately define individual geological layer thicknesses, conductivities, or depths to geological boundaries. To resolve those, the few-layer blocky model option is necessary but requires accurate estimations of the starting models number of layers and conductivity. The blocky model option has the ability to apply probabilistic constraints to each of the conductivity and thickness values in the starting model. These constraints restrict or penalize the inversion algorithm from deviating from the starting model values. Therefore, this additional method of constraining the inversion can be use when there is prior information about the geology, like well logs or boreholes.
For this survey, the inversion process began by using the multi-layer smooth option to model the final processed data. The starting model consisted of 33 layers with a starting thickness of 3.0 metres and grew logarithmically to a depth of 250 metres plus a basement layer. Each of these layers started from resistivity of 100 ohm-m. This inversion and each subsequent inversion run inverted every 10th sounding which results in a separation of 25-30 metres for each inverted model. The inversion was able to fit these models within the misfit for each of the soundings not heavily influence by cultural noise. The inversion model results were able to show the general structure of the geology's conductivity profile.

[2] https://github.com/GeoscienceAustralia/ga-aem
[3] Reid et al. 2006, Airborne electromagnetic footprints in 1D earths: Geophysics, 71, no. 2, pG63-G72.

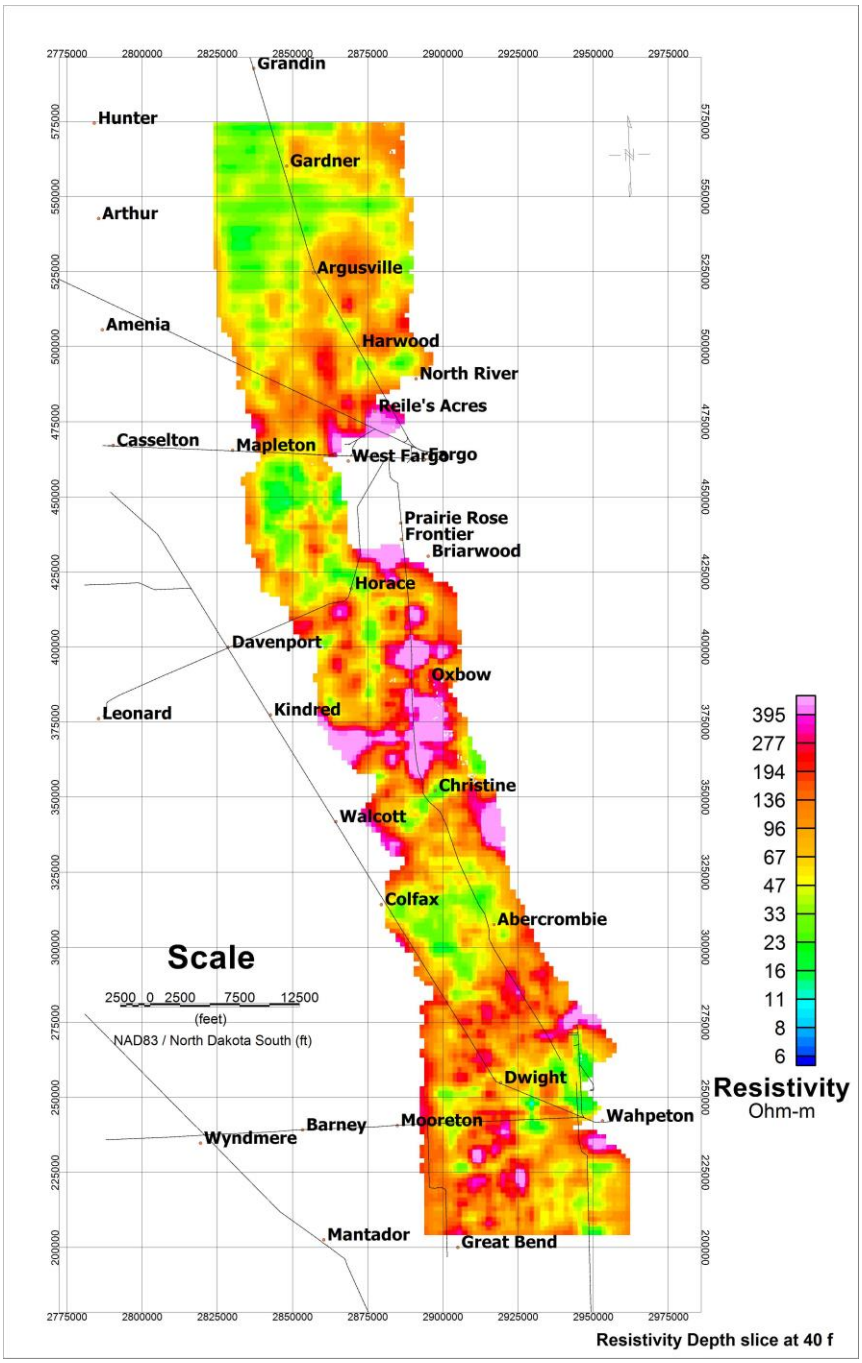

Figure 6: Resistivity Depth Slice at 40 ft from 1D unconstrained inversions

From the 1D inversion results, several products were generated which visualize the resistivity models in different perspectives. The products include: planar resistivity depth slices at 40 foot intervals, cross-sectional resistivity model for each flight line and tie line, and a 3D gridded voxel composed from each of the 1D resistivity inversion models which provides a 3D perspective of the resistivity variation across the entire survey block.

6. DELIVERABLES

6.1 SURVEY REPORT

The survey report describes the data acquisition, processing, 1D inversion modeling, and final presentation of the survey results. The survey report is provided in two paper copies and digitally in PDF format.

Aqua Geo Frameworks produced suvrey report that accompanies these survey results. The report titled: *Final Spatially-Constrained Inversions Report and Data Delivery for the Airborne Electromagnetic Survey of the Wahpeton, North Dakota Area for the North Dakota State Water Commission* focuses on the spatially constrained inversion and comparisons with borehole data.

6.2 MAPS

Final maps were produced at scale of 1:75,000 for best representation of the survey size and line spacing. The coordinate/projection system used was WGS84 Datum, UTM Zone 14 North. All maps show the flight path trace and topographic data; latitude and longitude are also noted on maps.

The preliminary and final results of the survey are presented as EM profiles, a late-time gate gridded EM channel, and a colour magnetic TMI contour map.

- Maps at 1:50,000 in Geosoft MAP format, as follows:

GL170349_75k_dBdt:	dB/dt profiles Z Component, Time Gates 0.021 – 0.880 ms in linear – logarithmic scale.
GL170349_75k_Bfield:	B-field profiles Z Component, Time Gates 0.021 – 0.880 ms in linear – logarithmic scale.
GL170349_75k_BFz36:	B-field time Z Component Channel 36, Time Gate 2.021 ms colour image.
GL170349_75k_TMI:	Total magnetic intensity (TMI) colour image and contours.
GL170349_75k_TotHGrad:	Magnetic Total Horizontal Gradient colour image.

- Maps are also presented in PDF format.
- The topographic data was derived from North Dakota GIS Hub Data Portal (https://gishubdata.nd.gov/), US Goverment Open Data (https://www.data.gov/) and Geocommunities (www.geocomm.com)
- A Google Earth file *GL170349_NDSWC.kmz* showing the flight path of the block is included. Free versions of Google Earth software from: http://earth.google.com/download-earth.html

6.3 DIGITAL DATA

Two copies of the data on DVD were prepared to accompany the report. Each DVD contains a digital file of the line data in GDB Geosoft Montaj format.

- DVD structure.

  Data contains databases, grids and maps, as described below.
  Report contains a copy of the report and appendices in PDF format.

Databases in Geosoft GDB format, containing the channels listed in Table 5.

Table 5: Geosoft GDB Data Format

Channel name	Units	Description
X:	metres	UTM Easting WGS84 Zone 14 North
Y:	metres	UTM Northing WGS84 Zone 14 North
Longitude:	Decimal Degrees	WGS 84 Longitude data
Latitude:	Decimal Degrees	WGS 84 Latitude data
Z:	metres	GPS antenna elevation
Zb:	metres	EM bird elevation
Radar:	metres	helicopter terrain clearance from radar altimeter
Radarb:	metres	Calculated EM transmitter-receiver loop terrain clearance from radar altimeter and two GPS elevations
DEM:	metres	Digital Elevation Model
Gtime:	Seconds of the day	GPS time
Mag1L:	nT	Measured Total Magnetic field data (left sensor)
Mag1R:	nT	Measured Total Magnetic field data (right sensor)
Basemag:	nT	Magnetic diurnal variation data
Mag2LZ	nT	Z corrected (w.r.t. loop center) and diurnal corrected magnetic field left mag
Mag2RZ	nT	Z corrected (w.r.t. loop center) and diurnal corrected magnetic field right mag
TMI2	nT	Calculated from diurnal corrected total magnetic field intensity of the centre of the loop
TMI3	nT	Microleveled total magnetic field intensity of the centre of the loop
Hginline		Calculated in-line gradient
Hgcxline		measured cross-line gradient
CVG	nT/m	Calculated Magnetic Vertical Gradient
PLM:		60 Hz power line monitor
SFz[4]:	pV/(A*m4)	Final Z dB/dt 0.021 millisecond time channel
SFz[5]:	pV/(A*m4)	Final Z dB/dt 0.026 millisecond time channel
SFz[6]:	pV/(A*m^4)	Final Z dB/dt 0.031 millisecond time channel
SFz[7]:	pV/(A*m^4)	Final Z dB/dt 0.036 millisecond time channel
SFz[8]:	pV/(A*m^4)	Final Z dB/dt 0.042 millisecond time channel

Channel name	Units	Description
SFz[9]:	pV/(A*m^4)	Final Z dB/dt 0.048 millisecond time channel
SFz[10]:	pV/(A*m^4)	Final Z dB/dt 0.055 millisecond time channel
SFz[11]:	pV/(A*m^4)	Final Z dB/dt 0.063 millisecond time channel
SFz[12]:	pV/(A*m^4)	Final Z dB/dt 0.073 millisecond time channel
SFz[13]:	pV/(A*m^4)	Final Z dB/dt 0.083 millisecond time channel
SFz[14]:	pV/(A*m^4)	Final Z dB/dt 0.096 millisecond time channel
SFz[15]:	pV/(A*m^4)	Final Z dB/dt 0.110 millisecond time channel
SFz[16]:	pV/(A*m^4)	Final Z dB/dt 0.126 millisecond time channel
SFz[17]:	pV/(A*m^4)	Final Z dB/dt 0.145 millisecond time channel
SFz[18]:	pV/(A*m^4)	Final Z dB/dt 0.167 millisecond time channel
SFz[19]:	pV/(A*m^4)	Final Z dB/dt 0.192 millisecond time channel
SFz[20]:	pV/(A*m^4)	Final Z dB/dt 0.220 millisecond time channel
SFz[21]:	pV/(A*m^4)	Final Z dB/dt 0.253 millisecond time channel
SFz[22]:	pV/(A*m^4)	Final Z dB/dt 0.290 millisecond time channel
SFz[23]:	pV/(A*m^4)	Final Z dB/dt 0.333 millisecond time channel
SFz[24]:	pV/(A*m^4)	Final Z dB/dt 0.383 millisecond time channel
SFz[25]:	pV/(A*m^4)	Final Z dB/dt 0.440 millisecond time channel
SFz[26]:	pV/(A*m^4)	Final Z dB/dt 0.505 millisecond time channel
SFz[27]:	pV/(A*m^4)	Final Z dB/dt 0.580 millisecond time channel
SFz[28]:	pV/(A*m^4)	Final Z dB/dt 0.667 millisecond time channel
SFz[29]:	pV/(A*m^4)	Final Z dB/dt 0.766 millisecond time channel
SFz[30]:	pV/(A*m^4)	Final Z dB/dt 0.880 millisecond time channel
SFz[31]:	pV/(A*m^4)	Final Z dB/dt 1.010 millisecond time channel
SFz[32]:	pV/(A*m^4)	Final Z dB/dt 1.161 millisecond time channel
SFz[33]:	pV/(A*m^4)	Final Z dB/dt 1.333 millisecond time channel
SFz[34]:	pV/(A*m^4)	Final Z dB/dt 1.531 millisecond time channel
SFz[35]:	pV/(A*m^4)	Final Z dB/dt 1.760 millisecond time channel
SFz[36]:	pV/(A*m^4)	Final Z dB/dt 2.021 millisecond time channel
SFz[37]:	pV/(A*m^4)	Final Z dB/dt 2.323 millisecond time channel
SFz[38]:	pV/(A*m^4)	Final Z dB/dt 2.667 millisecond time channel
SFz[39]:	pV/(A*m^4)	Final Z dB/dt 3.063 millisecond time channel
SFz[40]:	pV/(A*m^4)	Final Z dB/dt 3.521 millisecond time channel
SFz[41]:	pV/(A*m^4)	Final Z dB/dt 4.042 millisecond time channel
SFz[42]:	pV/(A*m^4)	Final Z dB/dt 4.641 millisecond time channel
SFz[43]:	pV/(A*m^4)	Final Z dB/dt 5.333 millisecond time channel
SFz[44]:	pV/(A*m^4)	Final Z dB/dt 6.125 millisecond time channel
SFz[45]:	pV/(A*m^4)	Final Z dB/dt 7.036 millisecond time channel
SFz[46]:	pV/(A*m^4)	Final Z dB/dt 8.083 millisecond time channel
SFx[20]:	pV/(A*m^4)	Final X dB/dt 0.220 millisecond time channel
SFx[21]:	pV/(A*m^4)	Final X dB/dt 0.253 millisecond time channel
SFx[22]:	pV/(A*m^4)	Final X dB/dt 0.290 millisecond time channel
SFx[23]:	pV/(A*m^4)	Final X dB/dt 0.333 millisecond time channel
SFx[24]:	pV/(A*m^4)	Final X dB/dt 0.383 millisecond time channel
SFx[25]:	pV/(A*m^4)	Final X dB/dt 0.440 millisecond time channel
SFx[26]:	pV/(A*m^4)	Final X dB/dt 0.505 millisecond time channel
SFx[27]:	pV/(A*m^4)	Final X dB/dt 0.580 millisecond time channel
SFx[28]:	pV/(A*m^4)	Final X dB/dt 0.667 millisecond time channel
SFx[29]:	pV/(A*m^4)	Final X dB/dt 0.766 millisecond time channel
SFx[30]:	pV/(A*m^4)	Final X dB/dt 0.880 millisecond time channel
SFx[31]:	pV/(A*m^4)	Final X dB/dt 1.010 millisecond time channel

Channel name	Units	Description
SFx[32]:	pV/(A*m^4)	Final X dB/dt 1.161 millisecond time channel
SFx[33]:	pV/(A*m^4)	Final X dB/dt 1.333 millisecond time channel
SFx[34]:	pV/(A*m^4)	Final X dB/dt 1.531 millisecond time channel
SFx[35]:	pV/(A*m^4)	Final X dB/dt 1.760 millisecond time channel
SFx[36]:	pV/(A*m^4)	Final X dB/dt 2.021 millisecond time channel
SFx[37]:	pV/(A*m^4)	Final X dB/dt 2.323 millisecond time channel
SFx[38]:	pV/(A*m^4)	Final X dB/dt 2.667 millisecond time channel
SFx[39]:	pV/(A*m^4)	Final X dB/dt 3.063 millisecond time channel
SFx[40]:	pV/(A*m^4)	Final X dB/dt 3.521 millisecond time channel
SFx[41]:	pV/(A*m^4)	Final X dB/dt 4.042 millisecond time channel
SFx[42]:	pV/(A*m^4)	Final X dB/dt 4.641 millisecond time channel
SFx[43]:	pV/(A*m^4)	Final X dB/dt 5.333 millisecond time channel
SFx[44]:	pV/(A*m^4)	Final X dB/dt 6.125 millisecond time channel
SFx[45]:	pV/(A*m^4)	Final X dB/dt 7.036 millisecond time channel
SFx[46]:	pV/(A*m^4)	Final X dB/dt 8.083 millisecond time channel
SFx	pV/(A*m^4)	Final Y dB/dt data for time channels 20 to 46
BFz	(pV*ms)/(A*m^4)	Final Z B-Field data for time channels 4 to 46
BFx	(pV*ms)/(A*m^4)	Final X B-Field data for time channels 20 to 46
BFy	(pV*ms)/(A*m^4)	Final Y B-Field data for time channels 20 to 46
SFxFF	pV/(A*m^4)	Fraser Filtered X dB/dt
SRawz	pV/(A*m^4)	Raw Z dB/dt data for time channels 4 to 46
SRawx	pV/(A*m^4)	Raw X dB/dt data for time channels 20 to 46
SRawy	pV/(A*m^4)	Raw Y dB/dt data for time channels 20 to 46
BRawz	(pV*ms)/(A*m^4)	Raw Z B-Field data for time channels 4 to 46
BRawx	(pV*ms)/(A*m^4)	Raw X B-Field data for time channels 20 to 46
BRawy	(pV*ms)/(A*m^4)	Raw Y B-Field data for time channels 20 to 46
SFltz	pV/(A*m^4)	Filtered Z dB/dt data for time channels 4 to 46
SFltx	pV/(A*m^4)	Filtered X dB/dt data for time channels 20 to 46
SFlty	pV/(A*m^4)	Filtered Y dB/dt data for time channels 20 to 46
BFltz	(pV*ms)/(A*m^4)	Filtered Z B-Field data for time channels 4 to 46
BFltx	(pV*ms)/(A*m^4)	Filtered X B-Field data for time channels 20 to 46
BFlty	(pV*ms)/(A*m^4)	Filtered Y B-Field data for time channels 20 to 46

Electromagnetic B-field and dB/dt Z component data is found in array channel format between indexes 4 – 46, X component data from 20 – 46, and Y component data from 20 – 46, as described above.

- Database of the VTEM Waveform "GL170349_AllWaveforms.gdb" in Geosoft GDB format, containing the following channels:

Table 6: Geosoft database for the VTEM waveform

Channel name	Units	Description
Time:	milliseconds	Sampling rate interval, 5.2083 microseconds
Tx_Current:	amps	Output current of the transmitter

- EM and Magnetic Data Grids in Geosoft GRD and GFX format, as follows:

BFz36:	B-Field Z Component Channel 36 (Time Gate 2.021 ms)
DEM:	Digital Elevation Model (metres)
CVG:	Calculated Vertical Derivative (nT/m)
PLM:	Power Line Monitor (60 Hz)
Hgcxline:	Measured Cross-Line Gradient (nT/m)
Hginline:	Measured In-Line Gradient (nT/m)
TMI3:	Total Magnetic Intensity (nT)
TotHgrad:	Magnetic Total Horizontal Gradient (nT/m)
Tiltdrv:	Magnetic Tilt derivative (radians)
SFz5:	dB/dt Z Component Channel 5 (Time Gate 0.026 ms)
SFz10:	dB/dt Z Component Channel 10 (Time Gate 0.055 ms)
SFz15:	dB/dt Z Component Channel 15 (Time Gate 0.110 ms)
SFz20:	dB/dt Z Component Channel 20 (Time Gate 0.220 ms)
SFz25:	dB/dt Z Component Channel 25 (Time Gate 0.440 ms)
SFz30:	dB/dt Z Component Channel 30 (Time Gate 0.880 ms)
SFz35:	dB/dt Z Component Channel 35 (Time Gate 01.760 ms)
SFz40:	dB/dt Z Component Channel 40 (Time Gate 3.521 ms)
SFz45:	dB/dt Z Component Channel 45 (Time Gate 7.036 ms)

A Geosoft .GRD file has a .GI metadata file associated with it, containing grid projection information. A grid cell size of 125 metres was used.

The EM 1D Inversion Models and products have been provided as follows:

- Final Inversion models in space delimited ASCII column data file, DAT format, with accompanied header files
- Planar resistivity depth slice grids at 40 foot intervals in Geosoft GRD and GXF formats
- Cross-section resistivity models for each line and tie line in Geosoft GRD and GXF formats
- 3D gridded resistivity voxel in Geosoft voxel and Geosoft XYZ format

6.4 FLIGHT VIDEO

Video was also recorded during the survey and is included in the final digital data.

7. CONCLUSIONS AND RECOMMENDATIONS

A helicopter-borne versatile time domain electromagnetic (VTEM™plus), horizontal magnetic gradiometer geophysical survey has been completed over the Wahpeton Project situated near Fargo, North Dakota.

The total area coverage is 1370 km^2. Total survey line coverage 2000 line kilometres. The principal sensors included a Time Domain EM system, horizontal magnetic gradiometer using two caesium magnetometers system. Results have been presented as stacked profiles, and contour colour images at a scale of 1:75,000.

The EM results were inverted in 1D by Geotech and again by Aqua Geo Frameworks performing laterally and spatial constraints on the inversions. Both sets 1D inversions show a strong correlation with the existing borehole information and were able to map the geological structure in the survey area, specifically Precambrian basement the Quaternary sands and gravels that represent aquifer material.

Respectfully submitted[4],

D. Danchenko

Dmitriy Danchenko
Geotech Ltd.

Keeme Mokubung
Geotech Ltd.

Geoffrey Plastow, P. Geo.
Data Processing Manager
Geotech Ltd.

Alexander Prikhodko, PhD, P.Geo
Director of Geophysics
Geotech Ltd.
January 2018

[4] Final data processing of the EM and magnetic data were carried out by Keeme Mokubung and Zihao Han from the office of Geotech Ltd. in Aurora, Ontario, under the supervision of Geoffrey Plastow, P.Geo. Data Processing Manager.

APPENDIX A

SURVEY AREA LOCATION MAP

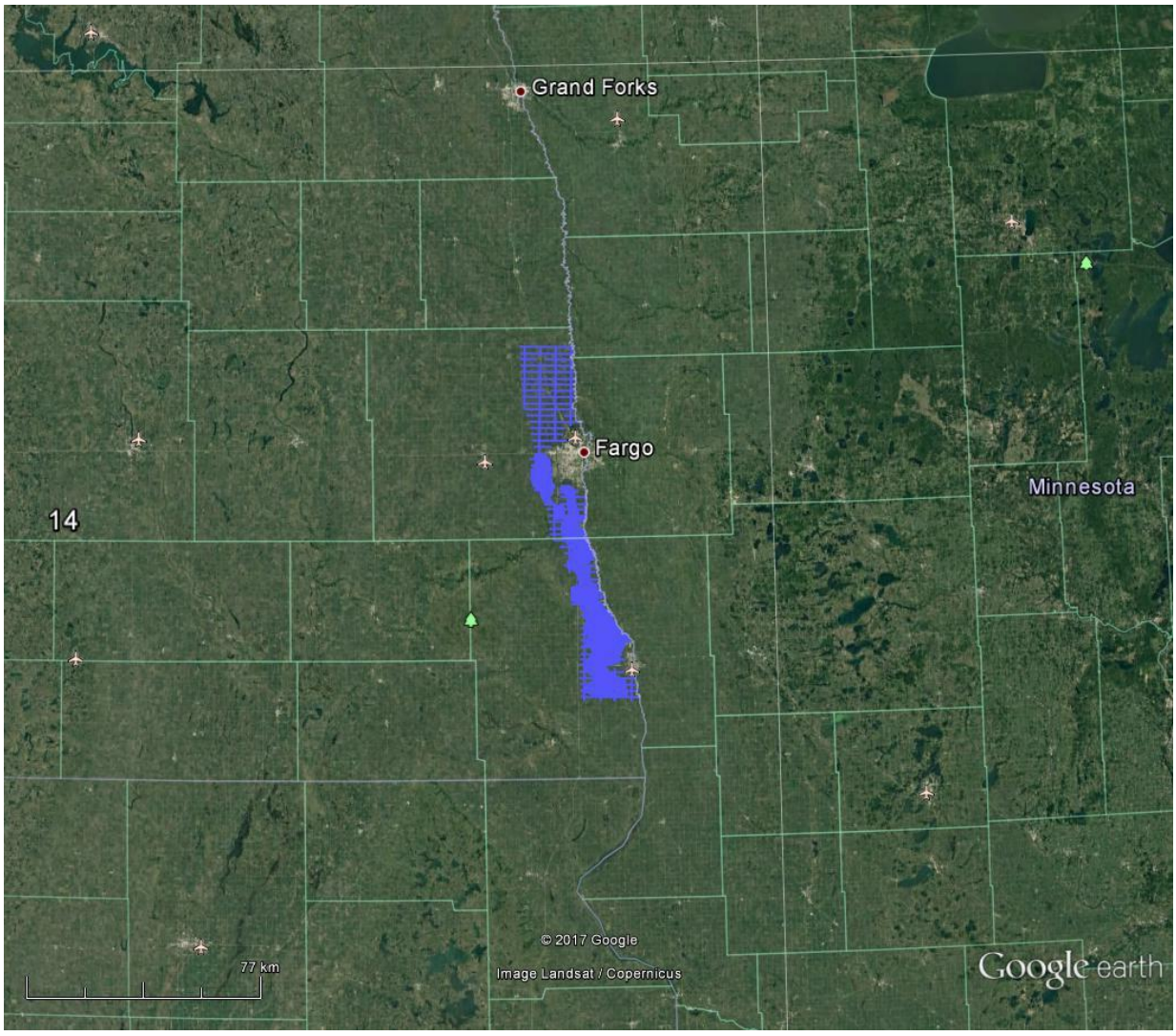

Overview of the Survey Area

APPENDIX B

SURVEY AREA COORDINATES

(WGS 84, UTM Zone 14 North)

WGS84 UTM Zone 14N		WGS84 UTM Zone 14N		WGS84 UTM Zone 14N		WGS84 UTM Zone 14N		WGS84 UTM Zone 14N	
X	Y	X	Y	X	Y	X	Y	X	Y
664960	5227920	655509	5179803	678127	5126088	669080	5168128	658832	5183852
647301	5227547	654549	5179803	681421	5126192	668764	5169665	657775	5183893
647841	5219863	654646	5179094	682193	5126764	666500	5169598	657626	5189938
648124	5214569	655709	5179100	682426	5126770	666462	5170557	658031	5190584
648706	5208886	655835	5178643	682386	5128135	666995	5171141	658088	5191207
654127	5211912	655875	5177466	681082	5128093	665902	5171213	656223	5192593
654119	5212711	656166	5177466	681073	5128333	665897	5171401	655040	5193443
656083	5212796	657071	5174250	681819	5128360	666199	5171406	655009	5194741
656089	5213627	657693	5167216	681800	5128949	666193	5171631	658033	5194833
657501	5213636	662217	5161872	681110	5128929	668428	5171702	657872	5196911
657819	5212802	665568	5156749	681096	5129280	668928	5171702	664331	5196911
656083	5212796	667123	5159989	681701	5129296	669583	5173940	664219	5198463
655662	5211925	667104	5160586	681682	5129881	669233	5179983	661534	5198438
654127	5211912	669069	5160608	684821	5129954	666446	5179994	661499	5200035
648706	5208886	669097	5160025	685014	5131436	666412	5180369	661888	5200087
650441	5203411	669229	5160025	681791	5131362	666786	5180457	661865	5200880
659267	5205679	669244	5159775	681720	5133330	666712	5182358	662219	5200926
659997	5205694	668084	5159770	684255	5133384	665979	5182337	662257	5201681
660146	5206140	668078	5159890	682719	5135722	665924	5182988	663587	5201694
661993	5206152	667488	5159872	674871	5130643	665241	5182954	666250	5201699
662018	5205828	667481	5159993	673234	5130643	665241	5183535	666546	5202176
661784	5205819	667123	5159989	673234	5129986	661641	5183535	667275	5202177
661800	5205284	665568	5156749	674871	5129986	660694	5180735	667213	5202294
661960	5205062	667031	5150942	674871	5130643	661224	5180716	667225	5203520
662158	5204336	667246	5148665	682719	5135722	661234	5180080	665866	5204458
660696	5204323	667521	5144095	680686	5137134	660817	5179976	665552	5206263
660315	5204694	667842	5139873	678620	5140989	660628	5177471	664621	5208291
659297	5204662	667843	5139756	676673	5143681	658867	5177461	665357	5210335
659267	5205679	669162	5139778	675838	5146076	658807	5179095	665657	5212018
650441	5203411	669183	5139060	673301	5146007	657636	5179085	665515	5215494
651498	5198562	667848	5139032	673273	5146664	657549	5179795	665759	5218909
652389	5194753	667902	5133676	675618	5146711	658653	5179800	664894	5220815
652023	5194753	667693	5129835	675127	5148786	658649	5180653	664424	5223168
652058	5193450	667436	5124474	674422	5149443	657955	5180685	664971	5225624
653223	5192593	667919	5114181	673780	5150628	657902	5181198	664960	5227920
653979	5190697	686905	5114289	673908	5152476	658601	5181206		
654286	5187075	685915	5120465	673220	5155435	658710	5181867		
655189	5181209	685159	5122643	673187	5157300	658328	5181955		
654909	5181209	685303	5123036	672743	5160200	658336	5182297		
655038	5180675	683277	5122982	672341	5161024	658633	5182341		
655275	5180695	683218	5125553	670818	5163447	658633	5183249		
655292	5180553	678140	5125476	669996	5165460	658903	5183293		

APPENDIX C

GEOPHYSICAL MAPS[1]

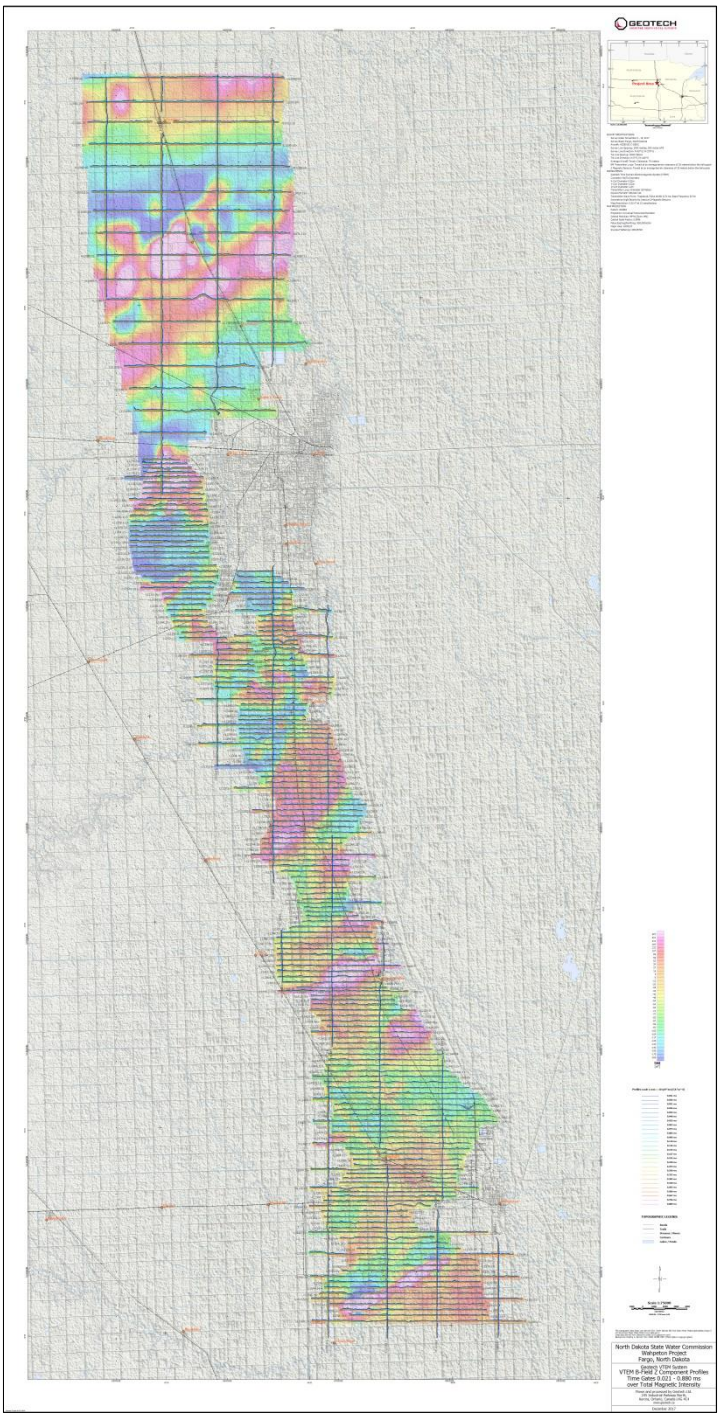

VTEM B-Field Z Component Profiles, Time Gates 0.220 to 7.036 ms

[1] Complete full size geophysical maps are also available in PDF format located in the final data maps folder

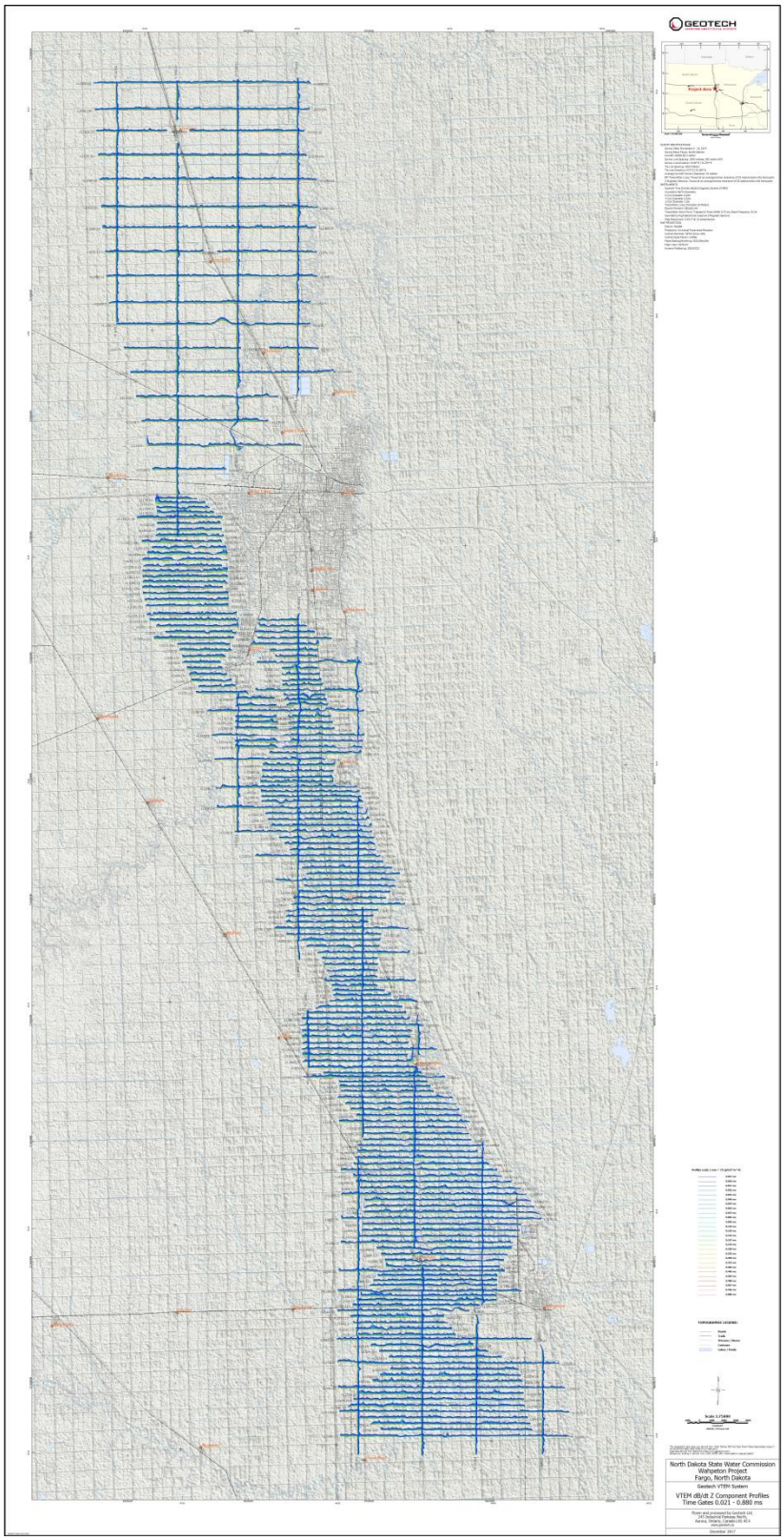

VTEM dB/dt Z Component Profiles, Time Gates 0.220 to 7.036 ms

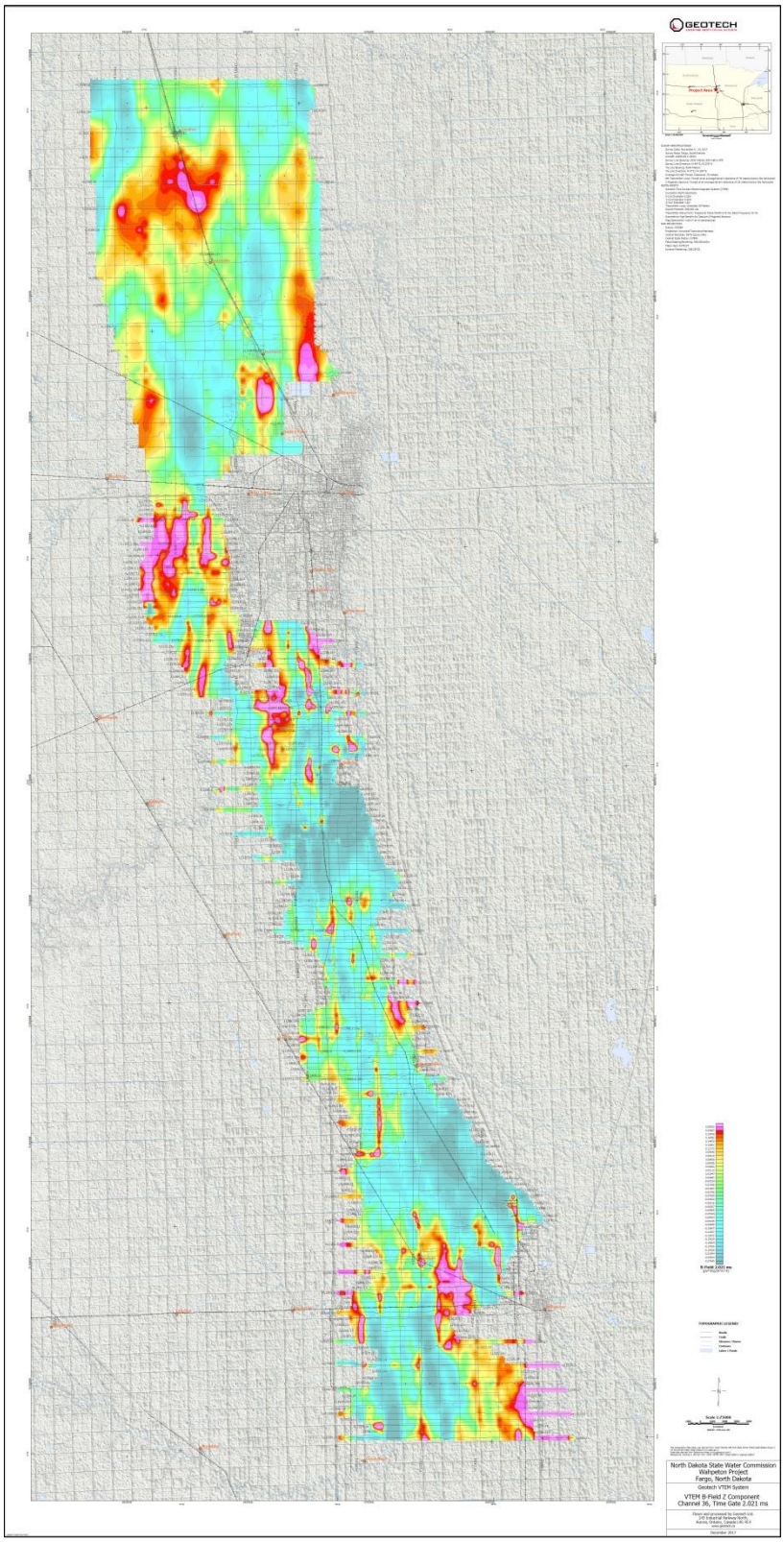

VTEM B-Field Z Component Channel 36, Time Gate 2.021 ms

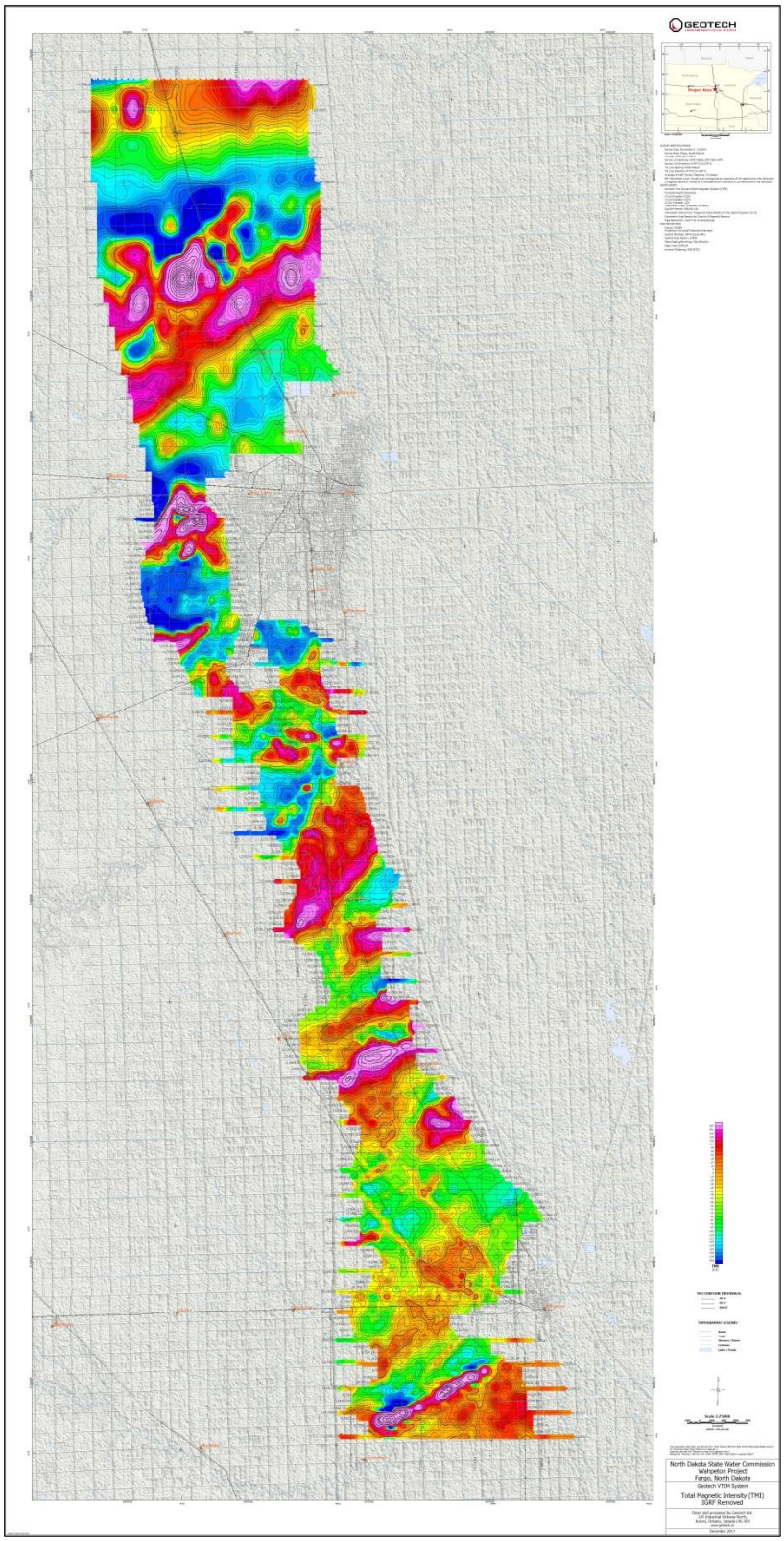

Total Magnetic Intensity (TMI)

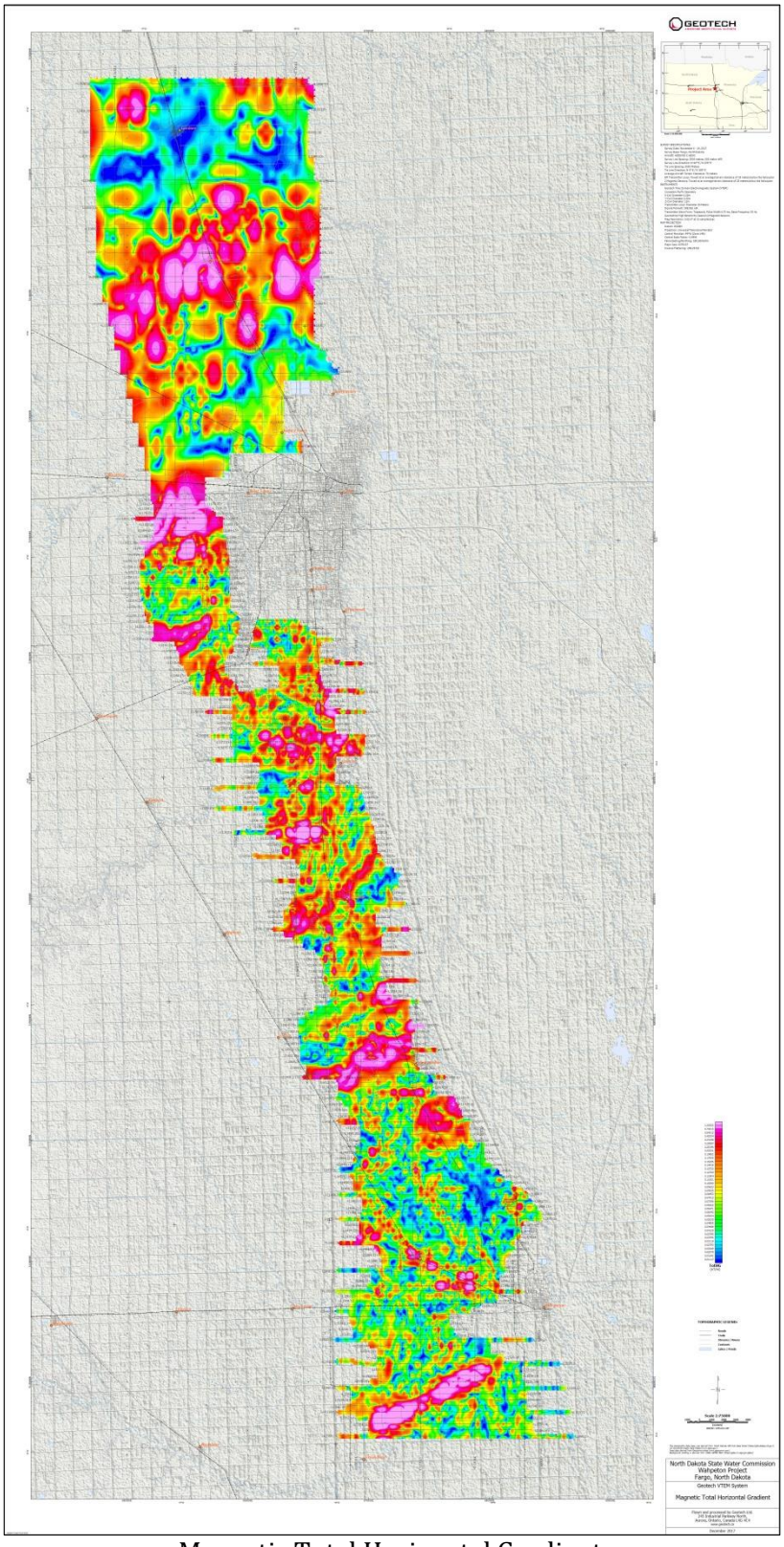

Magnetic Total Horizontal Gradient

APPENDIX D

GENERALIZED MODELING RESULTS OF THE VTEM SYSTEM
INTRODUCTION

The VTEM system is based on a concentric or central loop design, whereby, the receiver is positioned at the centre of a transmitter loop that produces a primary field. The wave form is a bi-polar, modified square wave with a turn-on and turn-off at each end.

During turn-on and turn-off, a time varying field is produced (dB/dt) and an electro-motive force (emf) is created as a finite impulse response. A current ring around the transmitter loop moves outward and downward as time progresses. When conductive rocks and mineralization are encountered, a secondary field is created by mutual induction and measured by the receiver at the centre of the transmitter loop.

Efficient modeling of the results can be carried out on regularly shaped geometries, thus yielding close approximations to the parameters of the measured targets. The following is a description of a series of common models made for the purpose of promoting a general understanding of the measured results.

A set of models has been produced for the Geotech VTEM™ system dB/dT Z and X components (see models D1 to D15). The Maxwell ™ modeling program (EMIT Technology Pty. Ltd. Midland, WA, AU) used to generate the following responses assumes a resistive half-space. The reader is encouraged to review these models, so as to get a general understanding of the responses as they apply to survey results. While these models do not begin to cover all possibilities, they give a general perspective on the simple and most commonly encountered anomalies.

As the plate dips and departs from the vertical position, the peaks become asymmetrical.

As the dip increases, the aspect ratio (Min/Max) decreases and this aspect ratio can be used as an empirical guide to dip angles from near 90º to about 30º. The method is not sensitive enough where dips are less than about 30º.

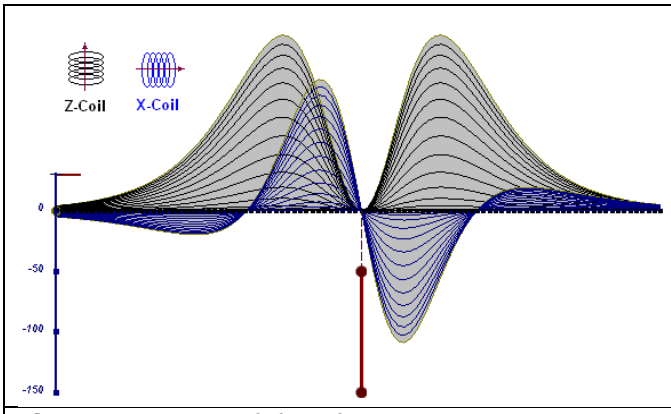

Figure D-1: vertical thin plate

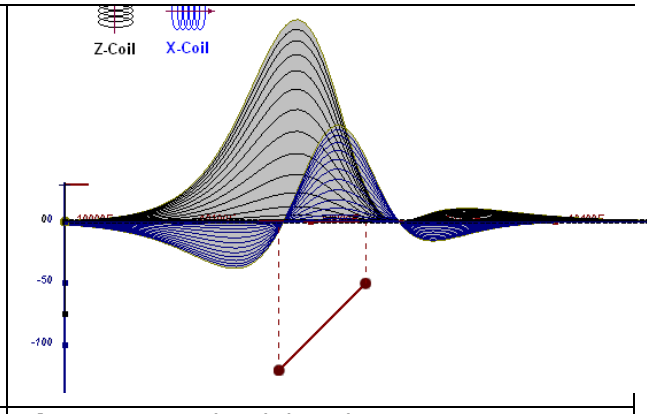

Figure D-2: inclined thin plate

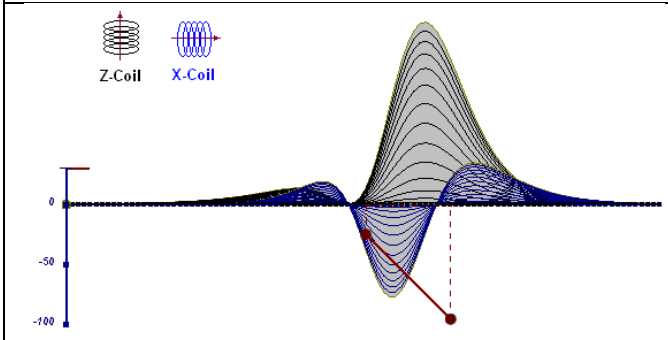

Figure D-3: inclined thin plate

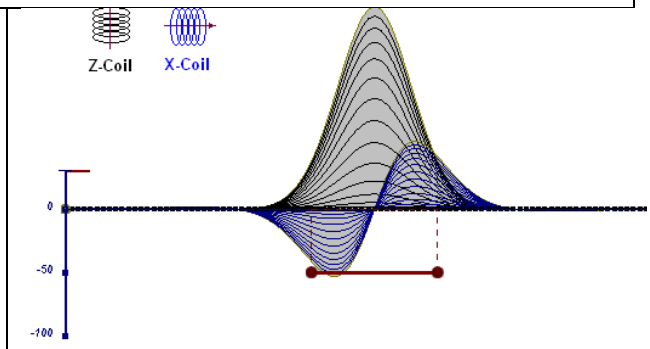

Figure D-4: horizontal thin plate

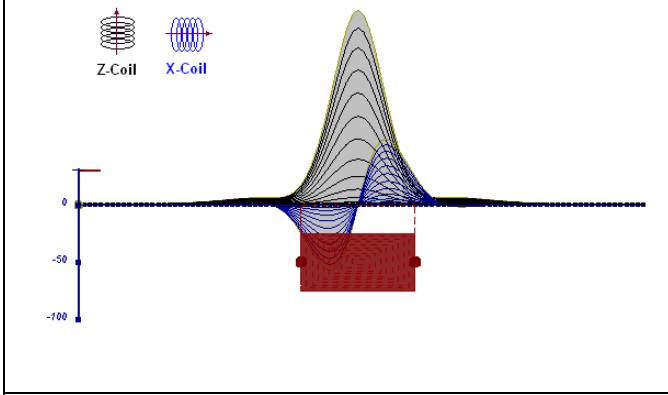

Figure D-5: horizontal thick plate (linear scale of the response)

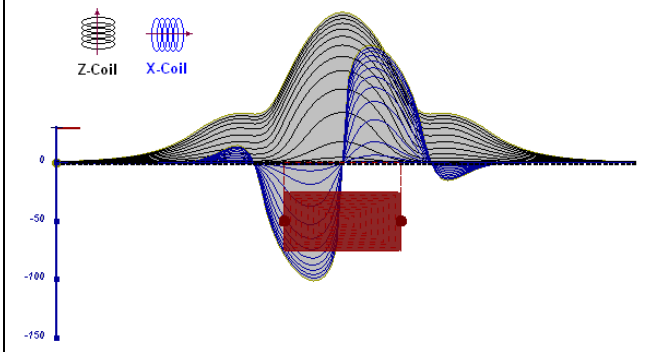

Figure D-6: horizontal thick plate (log scale of the response)

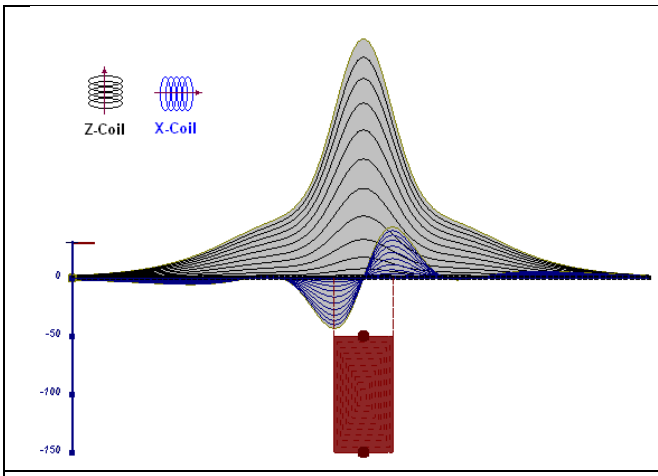

Figure D-7: vertical thick plate (linear scale of the response). 50 m depth

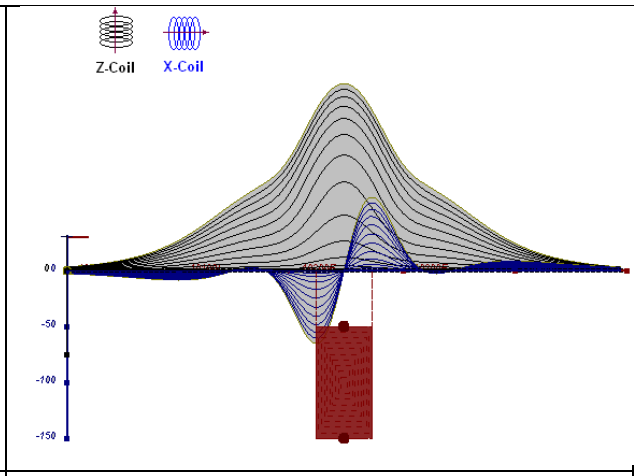

Figure D-8: vertical thick plate (log scale of the response). 50 m depth

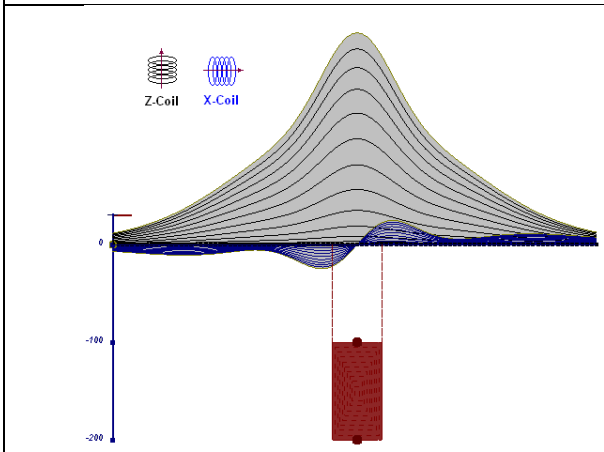

Figure D-9: vertical thick plate (linear scale of the response). 100 m depth

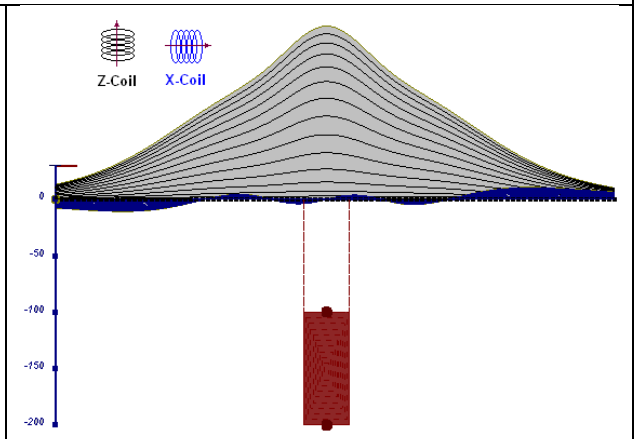

Figure D-10: vertical thick plate (linear scale of the response). Depth / horizontal thickness=2.5

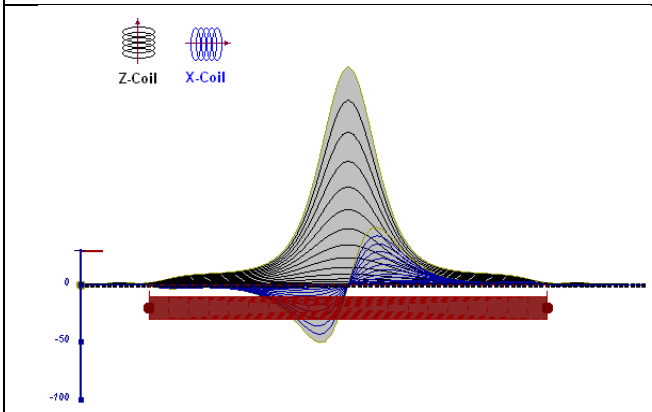

Figure D-11: horizontal thick plate (linear scale of the response)

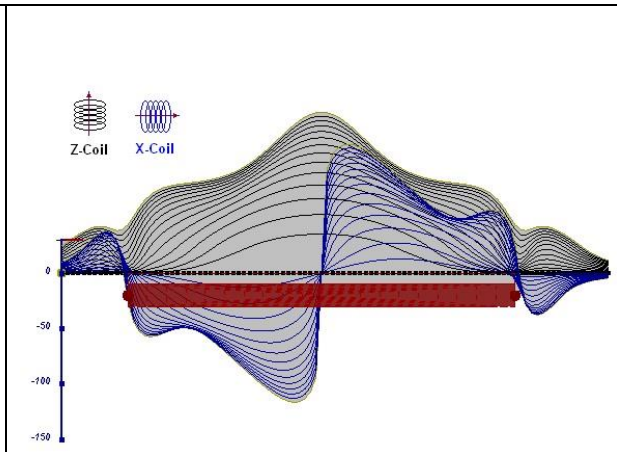

Figure D-12: horizontal thick plate (log scale of the response)

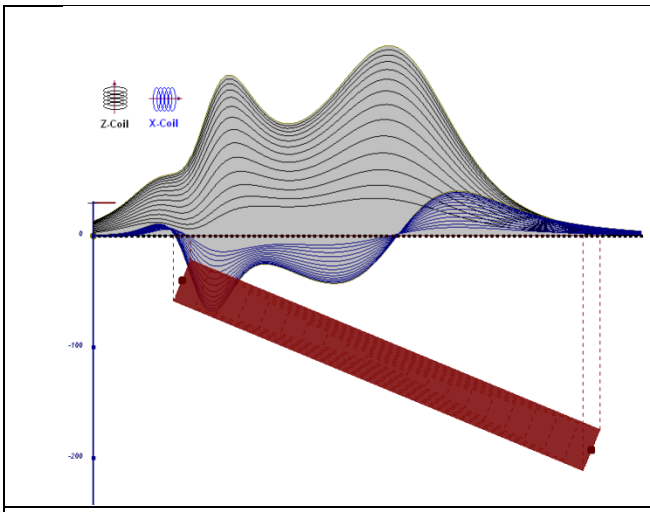

Figure D-13: inclined long thick plate

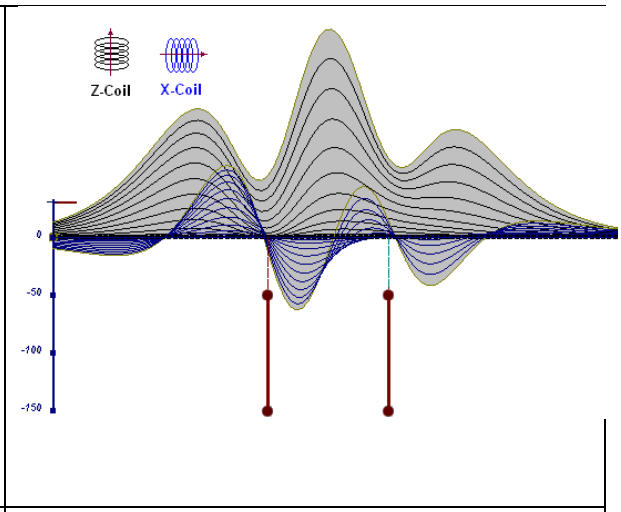

Figure D-14: two vertical thin plates

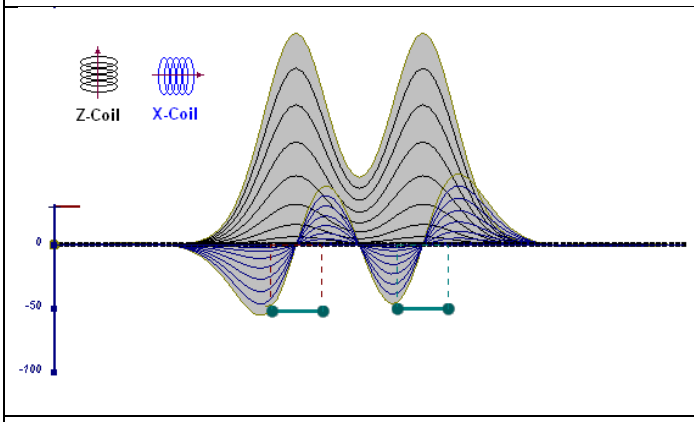

Figure D-15: two horizontal thin plates

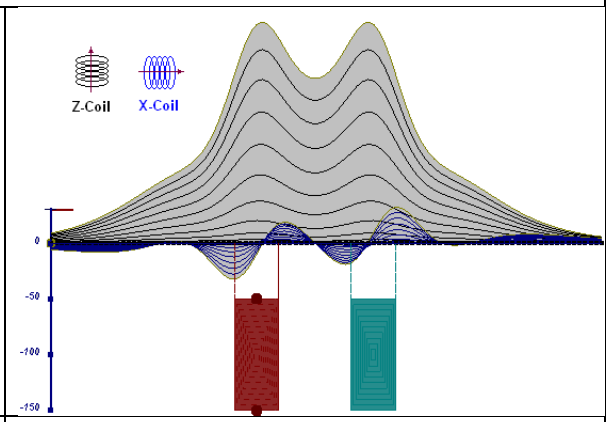

Figure D-16: two vertical thick plates

The same type of target but with different thickness, for example, creates different form of the response:

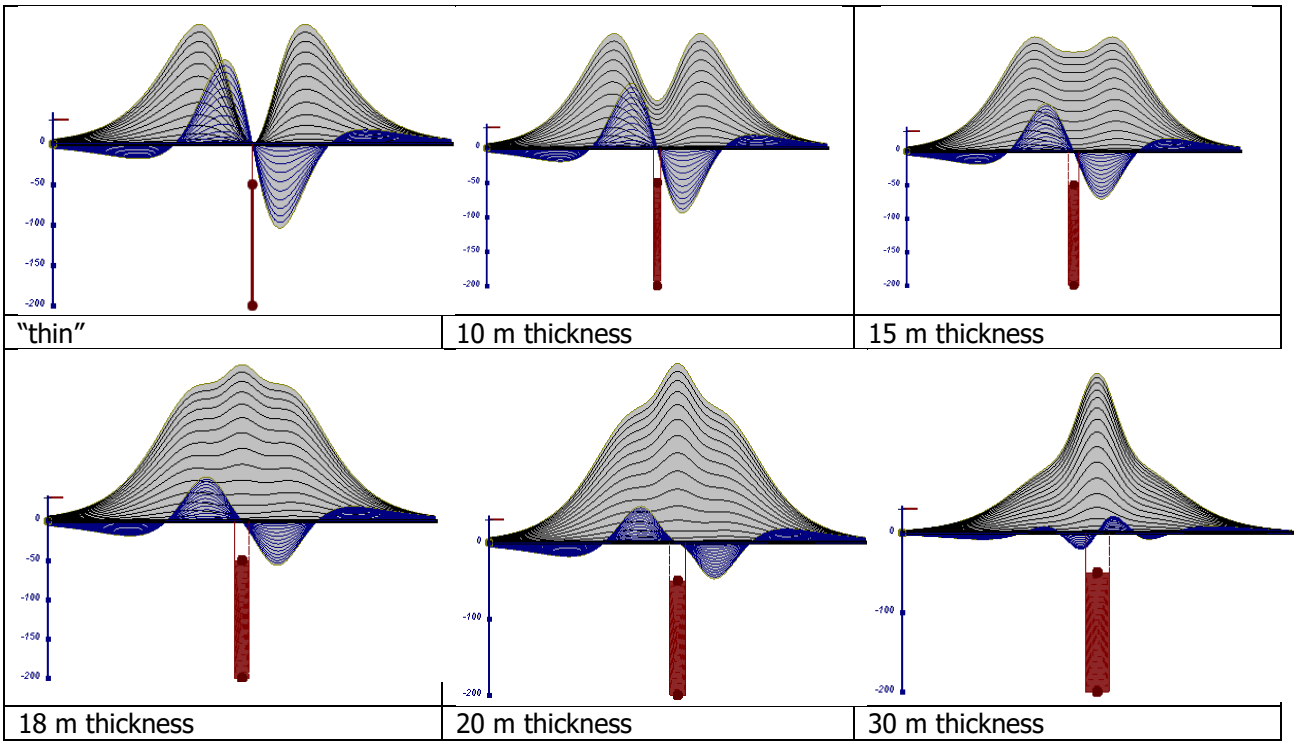

Figure D-17: Conductive vertical plate, depth 50 m, strike length 200 m, depth extends 150 m.

Alexander Prikhodko, PhD, P.Geo
Geotech Ltd.

September 2010